

Spring 5-1-2015

Pseudomonas Aeruginosa Elastase Induces Restructuring of Actin Cytoskeleton by Phosphorylation of RhoA Proteins

Bidisha Pal

Follow this and additional works at: https://scholarworks.uttyler.edu/biology_grad

 Part of the [Biology Commons](#)

Recommended Citation

Pal, Bidisha, "Pseudomonas Aeruginosa Elastase Induces Restructuring of Actin Cytoskeleton by Phosphorylation of RhoA Proteins" (2015). *Biology Theses*. Paper 24.
<http://hdl.handle.net/10950/265>

This Thesis is brought to you for free and open access by the Biology at Scholar Works at UT Tyler. It has been accepted for inclusion in Biology Theses by an authorized administrator of Scholar Works at UT Tyler. For more information, please contact tbianchi@uttyler.edu.

Pseudomonas Aeruginosa Elastase Induces Restructuring of Actin
Cytoskeleton by Phosphorylation of RhoA Proteins

by

BIDISHA PAL

A thesis submitted in partial fulfillment
of the requirements for the degree of
Masters of Science in Biology
Department of Biology

Ali O. Azghani, Ph.D., Committee Chair
College of Arts and Sciences

The University of Texas at Tyler
May 2015

The University of Texas at Tyler
Tyler, Texas

This is to certify that the Master's Thesis of
BIDISHA PAL
has been approved for the thesis requirement on
April 3, 2015
for the Masters of Science degree

Approvals:

Thesis Chair: Ali O. Azghani, Ph.D.

Member: James F. Koukl, Ph.D.

Member: Stephanie F. Daugherty, Ph.D.

Chair, Department of Biology

Dean, College of Arts and Sciences

© Copyright by Bidisha Pal 2015
All rights reserved

ACKNOWLEDGEMENTS

I would like to express my immense gratitude towards Dr. Ali Azghani for supervising my project entirely and coordinating my efforts towards the wholesome fulfilment of my thesis. His mentorship was paramount in providing me a well-rounded experience that was consistent with my long-term career goals. He encouraged me to not only grow as an experimentalist but also as an instructor and an independent thinker. I would take this opportunity to express my profound and deep regards to my committee members, Dr. Stephanie F. Daugherty and Dr. James F. Koukl, who have been instrumental in guiding me during the development of my research proposal and through the completion of this communication. I would also like to say my sincere and regardful thanks to Dr. Brent Bill, whose knowledge and expertise in Confocal Microscopy have helped me to improve the quality of the imaging data. I want to extend my thanks towards Dr. Srinu Kambhampati who gave me the opportunity to learn and grow as a researcher in this esteemed institution. I am also extremely thankful to all my Professors for guidance in various aspects of biology as well as my fellow graduate students for their extensive support and benevolence. Finally, and most importantly, I would like to thank GOD and my parents, allowing me to be as ambitious as I wanted. It was under their watchful eye that I gained so much drive and an ability to tackle challenges head on.

Table of Contents

List of Figures	iv
Abstract	viii
Chapter One	
Introduction.....	1
<i>Pseudomonas aeruginosa</i> , a Versatile Human Pathogen.....	1
Historical Relevance and Metabolic Adaptability	3
Infection Process.....	4
Virulence Factors	5
<i>Pseudomonas aeruginosa</i> Elastase	6-7
Impact of PE on Epithelial Permeability.....	8
Tight Junctions Complex.....	9-10
Interaction of PE with Tight Junction Proteins.....	11
Interplay of Signal Transduction Pathways	
EGFR Signaling Pathway.....	12-14
MAPK Signaling Pathway.....	14

RhoA GTPase Signaling Pathway.....	15-16
Interaction of RhoA GTPases with Actin Cytoskeleton.....	17
Hypothesis.....	17-18
Chapter Two	
Methods.....	19
Cell Culture.....	19
Biochemical and Immunological Assays.....	19-20
Fluorescence Microscopy.....	20
Specific Antibodies and Reagents.....	20
Treatment Protocols.....	21
Sample Preparation.....	21
Rho Activation Assay.....	21-23
Enzyme linked Immuno-Sorbent Assay.....	23-25
Biochemical Assay.....	25
Gel Electrophoresis.....	25
Western Blot Analysis.....	25-26

Immuno-staining.....	26-27
Statistical Analysis.....	27
Chapter Three	
Results	
Activation of RhoA GTPases by <i>Pseudomonas aeruginosa</i> Elastase.....	28-30
Inhibition of EGFR/MAPK Signal Transduction Pathway Attenuates PE-induced RhoA GTPase Activity.....	31-32
Quantitative Measurement of Total RhoA Proteins by ELISA Assay.....	33-35
PE alters Actin Cytoskeleton Architecture by RhoA Activation.....	36-37
Inhibition of RhoA/EGFR.MAPK Pathways Affects the Expression of ZO-1 Tight Junctional Protein.....	38-39
Chapter Four	
Discussion.....	40-46
Bibliography.....	47-60

List of Figures

Figure 1. Components of Tight Junction Complex.....	10
Figure 2. Schematic Representation of Cross Talk between EGFR-MAPK-Rho Signaling Pathways.....	12
Figure 3. Diverse Morphologies of Actin Cytoskeleton.....	16
Figure 4a. <i>Pseudomonas aeruginosa</i> Elastase Induces RhoA GTPase phosphorylation. Confluent monolayers of Calu- 3 were pre- treated with 500ng/ml of RhoA inhibitor for 120 minutes followed by stimulation with 3U/ml of PE for 5 minutes. PE induced RhoA GTPase phosphorylation was measured by G-LISA Small G- Protein Activation Assay. Data is expressed as means \pm standard deviation of triplicate assays. * indicate significant increase ($p=0.003$) in RhoA GTPase phosphorylation in PE treated cells in comparison to PBS-treated control cells. # indicates decrease in RhoA GTPase phosphorylation in RhoA inhibitor treated cells in comparison to PE treated Calu-3 monolayer.....	29
Figure 4b. <i>Concentration of Phosphorylated RhoA GTPase measured by G-LISA.</i> Confluent monolayers of Calu- 3 were pre- treated with 500ng/ml of RhoA inhibitor for 120 minutes followed by stimulation with 3U/ml of PE for 5 minutes. Data is expressed as means \pm standard deviation of triplicate assays. # indicate significant increase (<0.001) in RhoA GTPase phosphorylation in PE treated cells	

in comparison to PBS-treated control cells.* indicates decrease in RhoA GTPase phosphorylation in PE + RhoA inhibitor treated cells in comparison to PE- treated cells.....30

Figure 5. *Signal transduction pathways involved in PE induced RhoA GTPase Activity.* Confluent monolayers of Calu- 3 were pre- treated with 500ng/ml of RhoA inhibitor, 1 μ M EGFR inhibitor or 1 μ M of MEK inhibitor for 120 minutes and 15 minutes respectively, followed by stimulation with 3U/ml of PE for 5 minutes. PE induced RhoA GTPase phosphorylation measured by G-LISA Small G-Protein Activation Assay was found to be attenuated in presence of inhibitors. Data is expressed as means \pm standard deviation of triplicate assays. # indicate significant increase (p= 0.05) in RhoA GTPase phosphorylation in PE treated cells in comparison to PBS-treated control cells. * indicates decrease in RhoA GTPase phosphorylation in various inhibitor treated cells in comparison to PE - treated cells.....32

Figure 6a. *Concentration of Total RhoA protein in PE induced infection as measured by ELISA Assay.* Confluent monolayers of Calu- 3 were pre- treated with 500ng/ml of RhoA inhibitor, was stimulated with 3U/ml of PE for 5 minutes. ELISA measured the total amount of RhoA protein was expressed in cell lysates treated with both PE and PE with RhoA inhibitor. Data is expressed as means \pm standard deviation of triplicate assays. # indicate significant increase (p< 0.05) in

RhoA GTPase phosphorylation in PE treated cells in comparison to PBS-treated control cells. * indicates decrease in RhoA GTPase phosphorylation in RhoA inhibitor treated cells in comparison to PE- treated cells.....34

Figure 6b. *Concentration of Total RhoA protein in presence of various inhibitors as measured by ELISA Assay.* Confluent monolayers of Calu- 3 were pre-treated with 500 ng/ml of RhoA inhibitor, 1 μ M EGFR inhibitor or 1 μ M of MEK inhibitor for 120 minutes and 15 minutes respectively, followed by stimulation with 3 U/ml of PE for 5 minutes. Total amount of PE- induced RhoA protein was measured by ELISA Assay. Data is expressed as means \pm standard deviation of triplicate assays. # indicate significant increase ($p < 0.05$) in total RhoA in cell lysates treated with PE in comparison to PBS-treated control cells. * indicates decrease in the total concentration of RhoA protein in various inhibitor treated cells in comparison to PE- treated cells.....35

Figure 7. *Actin Cytoskeleton architecture is affected by PE induced RhoA GTPase activity.* Confluent Calu-3 monolayers were stained for F-actin where narrow arrows indicate formation of stress fibers, bold arrows indicate cell cortex and peripheries and arrow with double heads indicate formation of lamellipodium and triangle indicates filopodium. (A) In PBS treated cells, regular distribution of cell cortex and peripheries along with few stress fibers and lamellipodium was observed. (B) PE treatment (3 U/ml, 5 min) altered the cellular architecture and

induced formation of extensive stress fibers and lamellipodium. (C) RhoA inhibitor pre-treated cells restored the organization of cell cortex and regular lamellipodium. (D) EGF treated cells (positive control) caused similar reorganization of actin cytoskeleton by formation of stress fibers. (E) and (F) MEK inhibitor and EGFR inhibitor pre-treated cells reinstated the effect of PE by formation of cell cortex, lamellipodium and filopodium. Images are representative of triplicate assays and scale bar is 20 μm37

Figure 8. *Expression of ZO-1 is affected by attenuation of RhoA/EGFR and MAPK pathway.* Confluent monolayers of Calu- 3 were pre- treated with 500ng/ml of RhoA inhibitor, 1 μM EGFR inhibitor or 1 μM of MEK inhibitor for 120 minutes and 15 minutes respectively, followed by stimulation with 3U/ml of PE for 5 minutes. Proteins separated via SDS PAGE electrophoresis was transferred to Western Blot membrane. PE induces increase in RhoA GTP proteins in comparison to cells treated with inhibitors. The data from densitometry Analysis is observed to be insignificant (>0.05).....39

Abstract

Pseudomonas Aeruginosa Elastase Induces Restructuring of Actin Cytoskeleton by Phosphorylation of RhoA Proteins

Bidisha Pal

Thesis Chair: Ali O. Azghani, Ph.D.

The University of Texas at Tyler
May 2015

Pseudomonas aeruginosa causes aggressive infection in patients with pre-existing disorders and recurrent pulmonary infections in cystic fibrosis patients. Pathogenesis of *P. aeruginosa* infections is multifactorial owing to numerous virulence factors. The focus of this thesis research was to investigate whether *P. aeruginosa* elastase (PE) causes remodeling of the cytoskeleton by increasing the phosphorylation of RhoA GTPase proteins. In addressing our hypothesis, we utilized Small GTPase Immuno-sorbent Activation assays (G-LISA) and Enzyme linked Immuno-sorbent assay (ELISA) to quantitate changes in the total as well as phosphorylated RhoA protein in Calu3 cell lines. Fluorescence microscopy aided in understanding the changes in morphological

organization of F-actin. Changes in expression of TJ protein, ZO1, due to PE induced RhoA GTPase activity, was analyzed with SDS PAGE and Western Blot Analysis. Our data from G-LISA and ELISA assays indicate that PE increases the amount of active RhoA protein by 50.8% in comparison to PBS treated control cells. RhoA inhibitor reduced the PE-induced phosphorylation of RhoA proteins by 30.35 % in PE treated cells. Images from fluorescence microscopy revealed that increase in RhoA GTPase activity causes formation of specific morphological protrusions such as stress fibers, lamellipodium and filopodium. Presence of RhoA inhibitor reverses the changes induced by PE. Results from immunosorbent assays and fluorescence microscopy indicate that inhibition of EGFR and MAPK significantly reduces the PE-induced GTPase activity of RhoA by 48.07 % and 42.2 % respectively. Data from G-LISA and ELISA assays correlate well with the morphology data obtained by fluorescence microscopy. Taken together, our data indicate that PE, at least in part, activates RhoA kinase via upstream EGFR and downstream MAPK signaling pathways, in vitro. The impact of these PE-induced alterations in the anatomy and physiology of the tight junctional complex, and their impact on the homeostasis of the lungs, demands further investigation.

Chapter One

Introduction

Pseudomonas aeruginosa, a versatile Human Pathogen

Pseudomonas aeruginosa, a non-fermentative, aerobic, virulent pathogen from the family Pseudomonadaceae, is responsible for causing a wide range of community and hospital-acquired infections in diverse clinical settings (1, 2). *P. aeruginosa* rarely causes infection in the normal host, but when a local or general immunodeficiency arises, it proves to be an efficient opportunistic pathogen. *P. aeruginosa*-induced infections and pathologies often become more severe, damaging, and fatal in individuals with congenital immunodeficiency or with compromised immunity (2).

P. aeruginosa is considered as one of the most common and lethal pathogens responsible for ventilator-associated pneumonia (VAP) in intensive care units (3, 9). Compared with community-acquired strains, clinical isolates of *P. aeruginosa* tend to be resistant to multiple classes of antibiotics, making its treatment extremely complicated with a mortality rate of 38% (4). Ventilator-associated pneumonia continues to be a common cause of morbidity and mortality in critically ill patients, despite extensive research in the areas of prevention and management (5, 6). One of the important components of treating patients with pneumonia is the initial assessment of the severity of disease. The Acute Physiology and Chronic Health Evaluation II (APACHE II) score was first

developed to predict patient mortality at the time of admission to a critical care unit (7, 9). The APACHE II score at the time of diagnosis and admission is considered the best scoring system to predict mortality in patients with VAP. *P. aeruginosa* ranks second in causing infection among all pathogens reported to the National Nosocomial Infection Surveillance System as well as rating high in the European Prevalence of Infections in Intensive Care Study (8). Other sites of nosocomial infections by this pathogen include the urinary tract, the bloodstream, surgical site infections, and post burn skin injuries. Localized proliferation of bacterium at the burnt site may lead to systemic sepsis, which is often associated with a high degree of mortality (11). Studies conducted on burned-mouse model have shown that *P. aeruginosa* quorum-sensing systems, *las* and *rhl*, play an important role in the horizontal spread of the pathogen within burned skin, facilitate bacterial dissemination and contribute to its overall virulence (12).

The capacity of *P. aeruginosa* to produce such diverse, often overwhelming infections is due to the presence of an array of virulence factors (2). The low permeability of the cell wall of *P. aeruginosa* and its ability to efflux antimicrobial agents, make it intrinsically resistant to therapy. Furthermore, selection of the most appropriate antibiotic is often complicated by the ability of the pathogen to develop resistance to multiple antibacterial agents during the course of treatment (14). The combination of these factors enables the bacterium to display high levels of virulence and resistance to infection control in acute and chronic settings (15).

Historical Relevance and Metabolic Adaptability

The pathogen was first isolated in 1882 by a French chemist and bacteriologist Carle Gessard, through an experiment that identified this microbe due to its water soluble pigments that turned blue-green when exposed to ultra-violet light (13). The Gram-negative aerobic rod shaped pathogen is capable of growing and surviving in almost any environment but it lives primarily in water, soil, and vegetation (2). The ubiquitous nature of the microorganism reflects its ability to survive with minimal nutrition requirements. The tremendous amount of metabolic versatility to adapt and colonize in diverse niches that are often inhospitable to most other organisms, is mainly due to the large and complex genome of the gammaproteobacteria (16, 17). Further, it also reflects the extraordinary physiological capabilities and broad metabolic capacity of the *Pseudomonas aeruginosa* that, particularly in low-nutrient conditions, provides distinct advantages for outgrowing competitors (18).

The complete genome sequencing of wild type *P. aeruginosa* (PA01) has uncovered a great deal of useful information, concerning not only the various reasons for its pathogenicity but also revealing its potential for antibiotic resistance (19). Large number of genes for substrate uptake and catalysis have been identified which not only enable the bacterium to metabolize various compounds as nutrients but also facilitate high environmental adaptability (20).

In addition to environmental habitats, *P. aeruginosa* strains are also frequently isolated from clinical sources. It can colonize human body sites, with a preference for moist areas, such as the perineum, axilla, ear, nasal mucosa and

throat; it has also been isolated from the gastrointestinal tract. The organism colonizes the respiratory tract of mechanically ventilated patients, the gastrointestinal tract of patients receiving anticancer chemotherapy, and on the skin of burn patients (21, 22). The lung is a main target for colonization and infection by this bacterium, either in the context of a chronic, progressively deteriorating infection and inflammation in cystic fibrosis (CF) population, or in a more acute setting such as severe pneumonia in immunocompromised patients (23, 24).

Infection Process

Normally, in order to initiate the process of pathogenesis, *P. aeruginosa* must breach the normal cutaneous or mucosal barriers so as to substantially break the first-line of defenses of the human body. Such a break can result from either disruption of the junctional complex, interruption of the protective balance of normal mucosal flora by broad spectrum antibiotics, or alteration of the immunologic defense mechanisms such as chemotherapy-induced neutropenia or mucosal clearance defects in CF (2). Once *P. aeruginosa* colonizes the host tissues and systems such as the lungs, it promotes more pathologic changes including the obstruction of the host clearance mechanisms. The process helps the bacterium to establish itself within the host and transform to resist host defenses and antibiotic therapy (2). During the initial colonization phase, *P. aeruginosa* successfully utilizes its repertoire of virulence factors to manipulate local physiology and overcome host defenses. These virulence determinants aid the infectious process to progress either to a chronic infection phase

characterized by low production of extracellular virulence factors, or to an acute infection characterized by high production of cell-to-cell signaling dependent virulence factors (32-34). Flagella, pili, and lipopolysaccharide are not only important for motility and adhesion but also serve as activators of Toll-like receptor 5 (TLR5), TLR2, and TLR4, which may lead to hyper inflammatory response (26, 27). *P. aeruginosa* also has the ability to halt epithelial cell protein expression and kill host cells by using the ADP-ribosylating protein ExoA. The type III secretion system (T3SS) effectors which includes both ExoS and ExoT, are known for their ADP-ribosyl transferase and GTPase activating events (28, 29). They work in concert to inhibit actin polymerization, prevent blood cell migration and phagocytosis, and promote apoptosis (30). Along with other members of T3SS group, these virulence factors alter the epithelial layer by disrupting cell polarity, inducing damage, and preventing *P. aeruginosa* endocytosis and clearance from the respiratory tract (31).

Virulence Factors

Once the microbe invades the lung, it induces changes to reduce immune activation and obstruct clearance mechanisms for its persistence. *P. aeruginosa* employs a suite of secreted enzymes and immunosuppressing factors to dampen host immunity (35, 36). These harmful factors include elastase (encoded by LasB gene), LasA protease, and alkaline metalloprotease (aprA), and are assumed to play a major role during acute *P. aeruginosa* infection (37). The role of alkaline

protease in tissue invasion and systemic infections is unclear; however, its role in corneal infections could be substantial (38, 39).

Pseudomonas aeruginosa Elastase

LasB elastase, the protease of interest in this project, is a 33 KDa zinc metalloprotease, also known as pseudolysin or *P. aeruginosa* elastase (PE). It acts on proteins such as human and bovine elastin and collagen Type III and IV (41-44). Also, research has shown that elastase producing *P. aeruginosa* strains were able to degrade proteins from human wound fluids and human skin biopsies *ex vivo* (45). Although not all clinical isolates of *P. aeruginosa* produce PE, for those that do, the protease is an important candidate in delineating the pathogenic status of the microorganism. LasB elastase is highly efficient, with a proteolytic activity on elastin approximately 10 times that of *P. aeruginosa* alkaline protease. Also, its activity toward casein is approximately four times greater than that of trypsin (40). The ability of *P. aeruginosa* to destroy elastin protein is a major virulence determinant during acute infection since elastin is the major component of connective tissues in human and plays a key role in the functions of the lungs and vasculature (46, 40).

The concerted activity of two enzymes, LasB elastase and LasA elastase, is responsible for elastolytic activity which is believed to destroy elastin-containing human lung tissue and cause the pulmonary hemorrhages characteristic of invasive *P. aeruginosa* infections (40). Apart from its elastolytic activity, PE degrades fibrin and collagen. Also, it can inactivate substances such as human immunoglobulins G and A, airway lysozyme, complement

components, and substances involved in protecting the respiratory tract against proteases such as α -1-proteinase inhibitor, surfactant proteins (SP) and bronchial mucus proteinase inhibitor (40). Thus, PE is known not only to cause destruction of the tissue components but also to interfere with host defense mechanisms by degrading a number of components of the innate and adaptive immune systems. For instance, PE hydrolyses both surfactant proteins A and D, which mediate a variety of events in lung innate immunity (47- 49). Incubation of either *P. aeruginosa* or purified *Pseudomonas* elastase with cell free bronchioalveolar lavage (BAL) resulted in the degradation of SP- A. The degradative enzyme from *P. aeruginosa* was identified as elastase by ion trap mass spectroscopy followed by its purification by anion exchange chromatography (50). We have also reported that incubation of PE with purified monoclonal antibodies (mAb) reduces the intensity of both 55 and 25 KDa bands in a SDS PAGE gel (71).

Studies from our laboratory have confirmed the presence of PE in sputum samples of patients suffering from *P. aeruginosa* infection, using monoclonal antibody against PE (71). We have also reported that the purified *Pseudomonas* elastase increases paracellular permeability of epithelial linings in animal models of pulmonary edema (51, 52). We used *in vitro* model of epithelial paracellular permeability to understand the mechanism of action of PE in this phenomenon. Results of studies with primary cultures of alveolar type II pneumocytes indicated that PE enhances epithelial permeability by redistribution and/or degradation of tight junction proteins (53) (71). Similarly, *in vivo* studies done on guinea pigs showed an increase in lung epithelial permeability to macromolecules after

treatment with elastase (54). This increase in epithelial permeability was due to the disruption of the tight junctions between epithelial cells.

Studies with *P. aeruginosa* mutants deficient in elastase secretion have indicated that PE plays a major role in the pathogenesis of *Pseudomonas* infection in animal models. In an air pouch model in rats, the number of leukocytes, volume of exudate and the concentration of interleukin-8 was analyzed post injection of *P. aeruginosa* elastase. The number of neutrophils and the volume of exudate in the pouch cavity treated with PE increased significantly, which indicates its proactive role in inflammatory response in *Pseudomonas* infection (70). Taken together, this evidence of elastase-generated virulence suggests that genetic manipulation of elastase production or neutralizing the protease at the site of infection could theoretically ameliorate pulmonary exacerbations caused by *P. aeruginosa* infection.

Impact of PE on Epithelial Permeability

Increased epithelial permeability is a well-accepted consequence of mucosal inflammation on the outer surfaces of various internal organs. The epithelium plays an important role in inflammation by serving as an interface between invading pathogens, allergens, and particles while communicating with underlying immune system of the host (58). According to the data from American Lung Association, lungs are responsible for the purification of 8,000 - 9,000 liters of breathed-in air in the course of a single day. This astonishing volume of purified air finally combines with 8,000 - 10,000 liters of blood pumped in by the heart through the pulmonary artery to fuel the cells of the body. The lungs also

relieve the blood of their burden of waste and return a refreshed, oxygen-rich stream of blood to the heart through the pulmonary vein. Under physiological conditions, polarized epithelia form a protective barrier that allows regulated paracellular fluxes of solutes and nutrients as well as facilitates antigen sampling and surveillance by the mucosal immune cells. However, during inflammation, this protective mechanism becomes compromised by various stimuli from either side of the epithelial barrier. Various invading microorganisms try to gain an access into the host tissue by increasing the epithelial permeability on the apical (luminal) side by releasing a variety of agents such as pore forming toxins, cytoskeleton-modifying proteins, and bacterial lipopolysaccharide (LPS). While, on the basal side of the epithelial layer, activated immune cells try also induce barrier disruption so as to facilitate their movement to sites of pathogen invasion. In this occasion, mucosal immune cells release variety of pro-inflammatory cytokines such as interferon (IFN), tumor necrosis factor (TNF), and interleukin (IL)1 or releases particular proteases and reactive oxygen species (ROS) in order to gain access to the epithelia (59, 60). Hence, increased permeability across the airway epithelial barrier is a major contributor to pathogenesis of respiratory infection and inflammation and understanding the underlying mechanisms that control the epithelial barrier disruption is important in identifying molecular targets that modulate mucosal inflammation (58).

Tight Junctions Complex

Properties of the epithelium are regulated by adhesive interactions that occur at the cell–cell and cell–matrix contacts by junctional proteins and focal

adhesion complexes. These intercellular junctional complex comprises of adhesive and scaffolding proteins such as tight junctions (TJs), adherens junctions (AJs), desmosomes, and gap junctions. These proteins are anchored into different cytoskeletal structures such as actin filaments, intermediate filaments, and microtubules (58, 63).

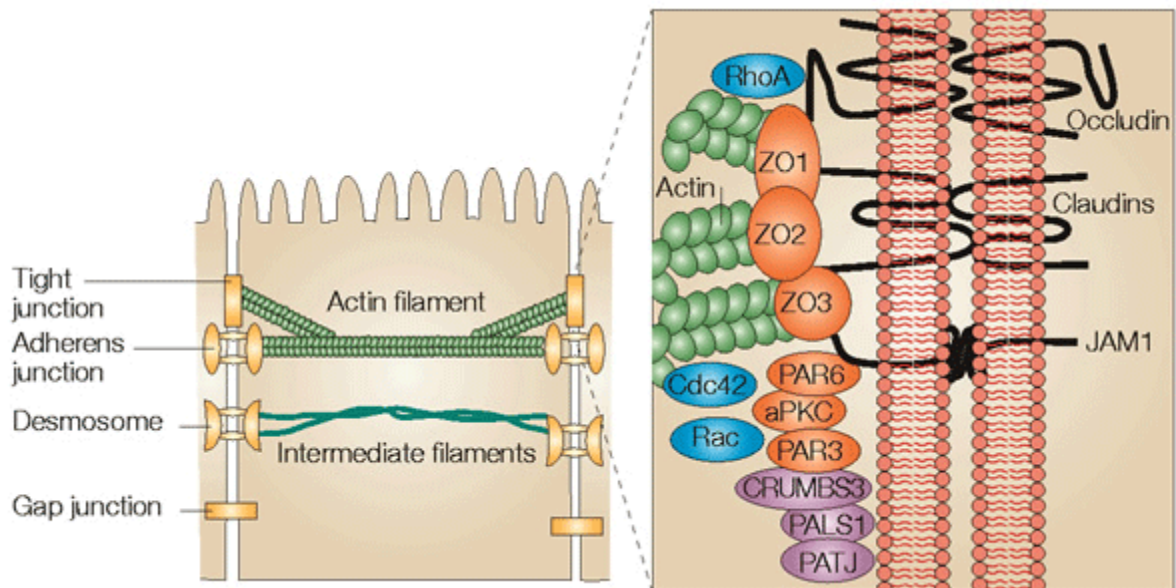


(Image credits: Klaus Aktories & Joseph T. Barbieri, May 2005)

Figure 1. Components of Tight Junction Complex

Tight junctions are highly dynamic structures and are constantly being remodeled in response to their interactions with external stimuli, such as allergens, pathogens, and commensal bacteria (61, 62). Proteins constituting the TJ complex include the transmembrane proteins occludin, junctional adhesion molecule (JAM), claudin family members, and linker proteins that affiliate with the underlying actin cytoskeleton. TJ complex is usually associated to belt like structure of peri-junctional filamentous actin (F-actin) molecules that encircles the

cells. This structure cooperates with TJ proteins in the regulation of trans-epithelial permeability or the 'gate function' of epithelial cells, and contributes to permeability regulation (64). These structures prevent the paracellular diffusion of macromolecules and microorganisms across the epithelial lining.

Interaction of PE with Tight Junction Proteins

Epithelial TJs are known to be influenced by a variety of endogenous and exogenous agents, including glucose, bacterial antigens, cytokines, and growth factors (65, 66, 67). During the process of inflammation, the apical junctions undergo the process of reorganization which in turn mediates epithelial barrier dysfunction. Such barrier dysfunction contributes to the pathogenesis of airway disorders such as asthma and acute lung failure. Defective epithelial barrier accelerates water influx into the lung which leads to pulmonary edema and further results in enhanced activation of the pulmonary and systemic immune responses by inhaled pathogens and allergens (68, 69). However, the mechanisms by which the external agents such as bacterial antigens, cytokines or growth factors signal to the TJs are not well understood.

Interplay of Signal Transduction Pathways

The transmission of extracellular signals to their intracellular targets is mediated by a network of interacting proteins that governs a large number of cellular processes. The modulation of TJ assembly and function could be via multiple signal transduction pathways including kinases, Ca^{2+} , G proteins, calmodulin, adenosine 3', 5'-cyclic monophosphate (cAMP), and phospholipase

C (72- 77). During bacterial infection, attachment of bacterium to host cells as well as extracellular virulence factors such as proteases, elicits responses in a variety of signal transduction pathways. These include the extracellular signal-regulated kinase (ERK) arm of the mitogen-activated protein kinases (MAPK) and epidermal growth factor receptor (EGFR) which in turn triggers the host inflammatory response against the existing infection. (87). Activation of these intracellular tyrosine kinase residues can initiate stimulation of signaling pathways via several adaptor proteins and protein kinases such as the Ras oncogene signaling pathway.

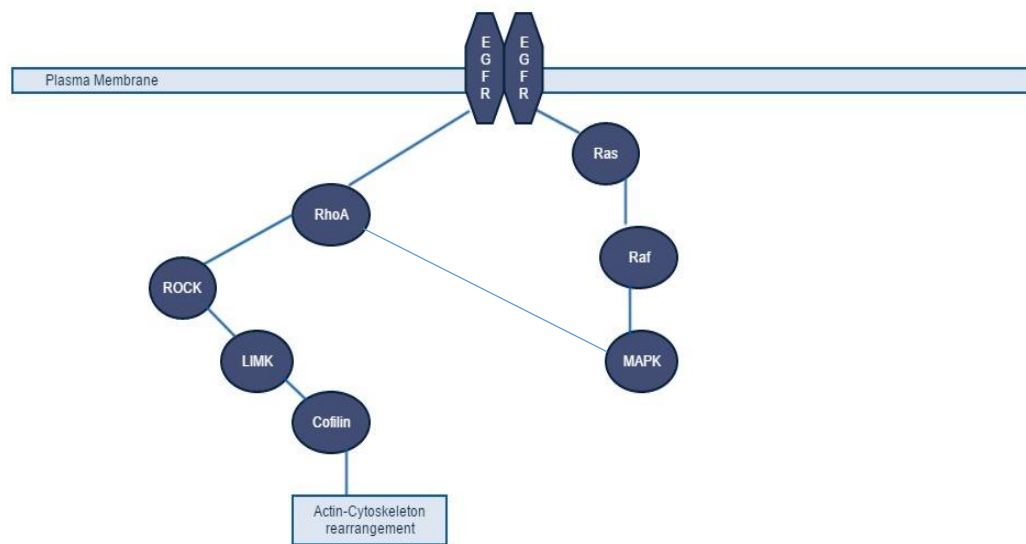


Figure 2. Schematic Representation of Cross Talk between EGFR-MAPK-Rho Signaling Pathways

EGFR Signaling Pathway

Epidermal growth factor receptor is a 170 kDa membrane glycoprotein, which belongs to the family of receptor tyrosine kinases that includes three other members, erbB2/HER-2, erbB3/HER-3, and erbB4/HER-4. The EGFR signaling

pathway is involved in a variety of physiological responses including proliferation, differentiation, motility, and survival (88). Receptor tyrosine kinases are composed of an extracellular ligand-binding domain, a short hydrophobic transmembrane region, and an intra-cytoplasmic tyrosine kinase domain. They share a similar structural homology with the other members of the family and are activated by multiple ligands including Epidermal growth factor (EGF), Transforming growth factor (TGF – α), heparin binding (HB)-EGF, amphiregulin, β -cellulin and epiregulin (89, 90). Activation of EGFR may involve two different pathways—ligand dependent and ligand independent EGFR tyrosine phosphorylation. Ligand independent EGFR phosphorylation is reported in response to cigarette smoke (91) and by activated neutrophils (92). Further analysis, however, revealed that the airway epithelial cells express EGFR pro-ligands on their surface along with the EGF receptors. Specific stimuli such as cigarette smoke can induce shedding of EGFR pro-ligands from the epithelial cell surface, leading to ligand dependent activation of EGFR signaling cascade. Likewise, neutrophils present in the airways of patients with hypersecretory diseases such as COPD, acute severe asthma, and cystic fibrosis could promote ligand independent EGFR activation and mucin synthesis. This ligand independent activation of EGFR occurs via the release of oxygen free radicals which raises the possibility of interactions between these cells and epithelial cells resulting in ligand dependent activation of EGFR signaling cascades (91, 92).

Previous studies from our lab indicate that PE induces activation of Protein Kinase C (PKC) signaling pathway through phosphorylation of Epidermal

Growth Factor Receptor (EGFR), which results in disruption of tight junction proteins, reorganization of the cytoskeleton, and destruction of epithelial barrier function (94).

MAPK Signaling Pathway

Mitogen-activated protein kinase (MAPK) pathways are evolutionarily conserved kinase modules that link extracellular signals to the machinery that controls fundamental cellular processes such as growth, proliferation, differentiation, migration and apoptosis. Currently, six distinct groups of MAPKs have been characterized in mammals which includes extracellular signal-regulated kinase (ERK) 1/2, ERK3/4, ERK5, ERK7/8, c-Jun N-terminal kinase (JNK)1/2/3 and the p38 isoforms. Historically, ERK signaling was synonymous with cell proliferation but it is now clear that dysregulation of this pathway is linked to many other aspects of the tumor phenotype. ERK signaling is activated by numerous extracellular signals as well as auto-phosphorylation of MEK and Raf (93). Activation of the MAP kinases-extracellular signal regulated kinases (MAPK/ERK) 1/2 has been associated not only with cell survival, proliferation, growth and differentiation but also with TJ protein disruption and cytoskeletal rearrangements. Previous studies from our lab have indicated that activation of the extracellular signal-regulated kinases (ERK) 1/2 arm of the mitogen-activated protein kinase (MAPK) pathway is involved in PE-induced TJ disruption (Azghani, unpublished data). Further, it was demonstrated that PE induces phosphorylation of ERK proteins within 5 minutes of apical exposure, preceded by a loss of

localization of TJ proteins occludin and ZO-1 along with the reorganization of the actin cytoskeleton (Azghani, unpublished data).

Recent advances in understanding the signaling pathways important for cytoskeletal rearrangements during cell migration have indicated that these pathways might have their relevance in the biogenesis and/or the maintenance of Tight Junctions. For example, the small GTP binding protein Rho regulates actin filament organization, and is important for the organization and permeability of the TJ in polarized epithelial cells (78). Also, most of the actin filaments are positioned under the apical junctional complex where myosin II and several actin binding proteins have been identified including α -actinin, vinculin, and radixin. This indicates the significance of actin binding proteins in the assembly and regulation of TJs and the associated reorganization of the architecture of the actin cytoskeleton (79).

RhoA Signaling Pathway

Rho family of small guanosine triphosphate (GTP)-binding proteins, one of the five distinct families of the Ras superfamily, has been shown to be important in the regulation of epithelial TJ structure, function, and assembly (80). The discovery of Rho protein was serendipitous in 1985 as a Ras-related protein (Ras homology) in *Aplysia*, and subsequently 18 genes encoding Rho-like proteins were identified in the human genome, with Rho, Rac and Cdc42 being the far best characterized (81, 82). The members of Rho family are small (21-25 kDa) molecules that act as molecular switches to regulate signal transduction pathways, by interconverting between inactive GDP-bound and active GTP-

bound conformational states. Studies have revealed the importance of Rho GTPases in regulation of various processes in reference to actin cytoskeleton including migration, phagocytosis, endocytosis, morphogenesis and cytokinesis. The first direct evidence that Rho and Rac regulate the assembly and organization of filamentous actin (F-actin) in response to extracellular cues was provided in 1992 (83, 84). In that study, Rho was shown to promote the assembly of contractile actomyosin filaments in response to lysophosphatidic acid (LPA) in a fibroblast cell line. In addition, Rac was shown to promote the assembly of a peripheral actin meshwork, leading to formation of lamellipodia and membrane ruffles in response to platelet-derived growth factor (PDGF) or insulin (83, 84).

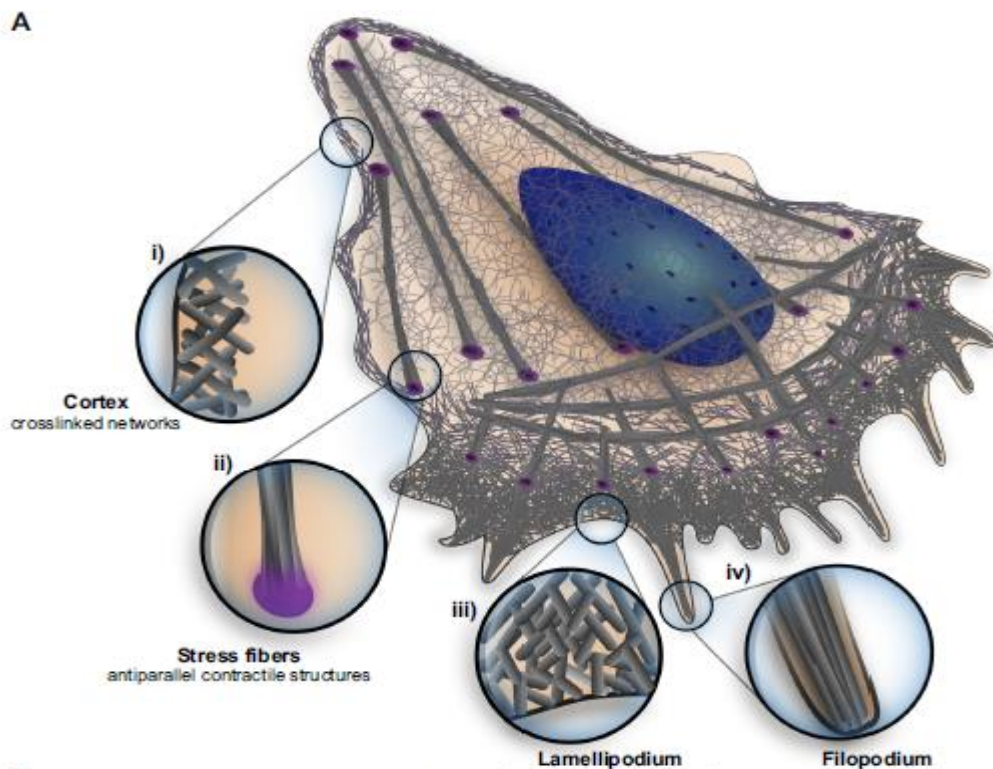


(Image credits: Laurent Blanchoin, Rajaa Boujemaa-Paterski, Cécile Sykes, and Julie Plastino, 2014)

Figure 3. Diverse Morphologies of Actin Cytoskeleton

Interaction of RhoA GTPases with Actin Cytoskeleton

Inactivation of Rho GTPases with *Clostridium botulinum* C3 transferase toxin or *Clostridium difficile* toxins A and B is associated with reorganization of F-actin in the perijunctional F-actin ring. These effects on the actin cytoskeleton were also shown to be accompanied by changes in TJ structure and function such as disruption of intercellular junctions. This results in the redistribution of VE-cadherin from the cell- cell contacts and formation of gaps in the monolayer (78). Additional studies using transfected epithelial cell lines expressing mutants of Rho GTPases have documented that Rho proteins play an important role in the regulation of TJ structure and function (85, 86). However, molecular mechanisms by which Rho proteins influence TJs of epithelial cells are not yet clear.

Hypothesis

In this study, we provide evidence in support of the hypothesis that *P. aeruginosa* elastase mediates activation of RhoA GTPases. We also sought to determine the cell signaling pathways that PE exploits in this process. We addressed our hypothesis by investigating that whether PE alters F-actin structure and organization by interconverting between the inactive GDP bound to active GTP bound conformational state of RhoA proteins. PE-induced RhoA activation was assessed by using Small GTPases linked Immuno-sorbent assay (G- LISA). Total RhoA was quantitated by Enzyme-linked immuno-sorbent assay (ELISA). We confirmed our immunochemical data by fluorescence microscopy. We found that PE-induced phosphorylation of RhoA proteins, a

downstream mediator of Rho-ROCK (Rho-associated kinase) signaling pathway, causes restructuring of the actin cytoskeleton. Further, we explored the molecular mechanisms that PE exploits to phosphorylate RhoA intermediate in Rho-ROCK signaling cascade. Our data revealed that that PE activates RhoA through EGFR and MAPK signaling pathways. These findings were further supported by the morphological analysis of Calu-3 monolayer treated with specific inhibitors of EGFR and MAPK.

Chapter Two

Material and Methods

I. *Cell Culture*: We used a human bronchial adenocarcinoma epithelial cell line (Calu-3) from American Type Culture Collection (ATCC, Manassas, Virginia), as an *in vitro* model to understand the role of *Pseudomonas* Elastase (PE) induced RhoA GTPases activity in cytoskeleton reorganization, Tight Junction (TJ) proteins disruptions and increased epithelial permeability leading to pulmonary edema . The cells were cultured and maintained in Dulbecco's Modified Eagle's Medium (Gibco, Life Technologies, Grand Island, NY) at 37°C in humidified atmosphere of 5% CO₂ / air. The medium was supplemented with 10% Fetal Bovine Serum (FBS; Atlanta Biologicals, Lawrenceville, GA), 1% L-glutamine (Cellgro, Herndon, VA) and cocktail of antibiotics containing Penicillin (100 U/ml), streptomycin (0.1mg/ml), and Amphotericin B (25 µg/ml), all from Cellgro, Herndon, VA. Cells were maintained in tissue culture flasks (Corning, Corning, NY) and were discarded at passage numbers 20. The medium for the flasks was changed every other day to avoid nutrient depletion. We used trypsin/EDTA (0.25%, Gibco, Life Technologies, Grand Island, NY) to transfer the cells from flasks to the appropriate cell culture ware according to the experimental design:

a. Biochemical and Immunological assays: We utilized different assays for understanding the PE induced RhoA GTPases activity in Calu-3 cell lines. For experimental purposes, cells were plated at high density (250,000 cells/well) in 6-

well tissue culture plates (Corning, Costar). The cells density/well was kept high so they reach confluency within short interval of time.

b. Fluorescence Microscopy: For analyzing the morphological changes in actin cytoskeleton, Calu-3 cells, at 8×10^5 cells/well, were cultured on 8 - well chamber slides (Lab-Tek, Rochester, NY). Calu-3 cells were grown to 80 % confluence in complete medium containing 10% FBS. Prior to treatments, the serum content in the medium was dropped gradually from 10% to 1% within a time interval of 12 hours followed by a complete serum starvation for 6 hours.

II. *Specific Antibodies & Reagents*: We used purified *P. aeruginosa* elastase (Elastin Product Co, Owensville, MO) as the primary bacterial toxin in this project. The purity and enzymatic activity of *P. aeruginosa* elastase (PE) was confirmed by using an elastin-fluorescein assay as directed by the manufacturer. One unit of purified *P. aeruginosa* elastase will hydrolyze 1 μ gm insoluble elastin per hour at 37°C. Elastase was applied apically on Calu-3 monolayers at a concentration of 3 U/ml.

Specific inhibitors of EGFR and MAPK pathways were utilized to understand the significance of various signal transduction pathway involved in PE-induced RhoA activation. These reagents include “EGFR inhibitor AG1478” (Calbiochem, La Jolla, CA, USA), “MEK 1&2 inhibitor U0126” (Calbiochem, La Jolla, CA, USA) and Rho inhibitor I (CTO4) (Cytoskeleton, Inc., Denver, CO). The product CTO4, with molecular weight of 24 kDa, is based on the exoenzyme C3 Transferase from *Clostridium botulinum* which has been covalently attached to a proprietary cell penetrating moiety.

III. *Treatment Protocols*: Cells were pre-treated for 15 minutes with 1 μ M of either “EGFR inhibitor AG1478” or “MEK 1&2 inhibitor U0126” or with 500ng/ml of Rho Inhibitor for 2 hours prior to PE exposure. As a positive control, we treated the cells with Human thrombin (Sigma, St. Louis, MO) or Human recombinant Epidermal Growth Factor (EGF) (R&D Systems, Inc., MN) for 10 minutes. All inhibitors were diluted in serum free DMEM. Solutions prepared for different treatments were then utilized in various biochemical, morphological and functional assays.

IV. *Sample Preparation*

Rho Activation Assay: The Small GTPases linked Immuno Assay (G-LISA) (Cytoskeleton, Inc., Denver, Colorado, USA) was utilized to detect the active form of Rho proteins in cell lysates. Calu-3 cells were grown to 80% confluence in 6 well tissue culture plates in complete media (DMEM) containing 10% FBS. The serum content in the medium was dropped gradually from 10% to 1% within a time interval of 12 hours followed by a complete serum starvation for 6 hours. Cells were then treated with the following mediators in the absence of serum. Thrombin (1.0 U/ml), PE (2.0 - 3.0 U/ml), EGFR inhibitor (10 μ M/ml), Erk1/2 inhibitor (10 μ M/ml) and Rho Inhibitor I (0.5 μ g/ml). Upon stimulation for 5 min at 37°C, we rapidly processed the cell lysates as follows.

The culture plate was placed on ice to aspirate off the culture medium and cells were washed with ice cold PBS. The cells were lysed by using 70 μ l of ice cold Cell Lysis Buffer while keeping the culture plate on ice. The cell lysates were then harvested by using a cell scraper (Sarstedt AG & Co., Nümbrecht,

Germany) and transferred to pre-labeled micro-centrifuge tubes on ice. The lysates were clarified by centrifugation at 10,000 x g at 4 °C for 1 minute. We used 10 µl of cell lysates for protein quantitation process while rest of the lysates were saved in aliquots at -70 °C. If the sample variation amongst the cell lysates was more than 10%, following formula was used for the normalization of the protein samples by adding ice cold Cell Lysis Buffer to more concentrated samples:

$$A - B/B \times \text{volume of A} = V \text{ (Volume of Lysis Buffer to be added)}$$

[where A is the higher concentration lysates (mg/ml) and B is the concentration of the most dilute sample (mg/ml)].

Once the cell lysate concentration was normalized, lysis buffer was diluted with ice cold binding buffer to prepare buffer blank while positive control for the assay was prepared by diluting GTP- RhoA protein with lysis buffer and ice cold binding buffer in a pre-labeled micro-centrifuge tube and utilized within 15 minutes as it will be denatured otherwise. Required number of 96-well strips were then placed on strip holder on ice and the powder in the wells was dissolved by adding 100 µl ice cold sterile water. Immediately, frozen lysates were thawed out by moving them in room temperature water bath and then subsequently transferred to ice. In order to ensure avoidance of high background noise, we applied a series of 5-7 vigorous pats of plate prior to the removal of solution from the wells. This was followed by the pipetting of normalized cell lysates and the ice cold binding buffer along with the positive control and buffer blank for the group into the respective wells. Immediately the plate was placed on a vortex

mixer (Fisher Scientific, Waltham, MA) at 4°C for 30 minutes at 400 rpm. The solution was then removed and the wells were washed twice with wash buffer by using multi-channel pipette. The antigen presenting buffer was then added into each well, followed by a 2 minute incubation at room temperature. This step is followed by removing the solution and immediate washing of wells at room temperature thrice with wash buffer as outlined above. All the wells were incubated with primary antibody diluted in antibody dilution buffer while keeping the plate on shaker at 400 rpm for 45 minutes at room temperature. Post incubation with primary antibody, the solutions were flicked out and the wells were washed with wash buffer thrice at room temperature. Secondary antibody dilution was prepared with antibody dilution buffer prior to addition into the wells and the plate was incubated for 45 minutes at orbital shaker at 400 rpm in room temperature. This was followed by removing solutions from the wells and washing thrice with wash buffer. Finally, horseradish peroxidase enzyme (HRP) detection reagent solution was added into each well followed by incubation of the plate at 37°C for 15 minutes. At the end of the reaction, HRP stop buffer was added and the absorbance signal was measured at OD₄₉₀ nm using AD340 spectrophotometer and analysis software (Beckman Coulter, Brea, CA).

V. Enzyme-linked Immuno-sorbent Assay (ELISA) for Total RhoA measurement:

The Total RhoA ELISA Assay Kit (Cytoskeleton, Inc., Denver, CO) was used for the quantitative measurement of RhoA in cell extracts. The kit is a highly selective sandwich ELISA format where each well is pre-coated with anti-Rho IgY antibody with a high affinity for Rho isotypes. The presence of RhoA in sample

lysates will allow its binding to the bottom of well. This step is followed by treatment with monoclonal antibody and its subsequent detection by secondary antibody- HRP conjugate and the substrate. Before the cell lysate are thawed out, four different concentrations of positive control was prepared for the assay in a pre-labeled micro-centrifuge tube. The thawed cell lysates were then mixed with sample dilution buffer into separated micro-centrifuge tubes. Required numbers of wells were placed on strip holder plate on ice. The powder in the wells were dissolved by adding 100 μ l M Q water at room temperature. Once the powder in wells was dissolved, the solution from the wells were completely removed. This requires series of 5-7 vigorous flicks of the plate onto paper towels so that the high background noise in the wells could be avoided. This was followed by the pipetting of equalized cell lysates into the respective wells for a period of 2 hour incubation at room temperature. The solution was then removed and the wells were washed twice with wash buffer by using multi-channel pipette. The antigen presenting buffer was then added into each well for 2 minute at room temperature. This step is followed by flicking out the solution and immediate washing of wells at room temperature thrice with wash buffer. This is followed by the incubation of wells with primary antibody for 60 minutes at room temperature. The solutions were removed and the wells were washed with wash buffer thrice at room temperature. Incubation with secondary antibody was performed for another 60 minutes in room temperature. This is followed by the flicking out of solutions from the wells and washing thrice with wash buffer. Finally, HRP detection reagent solutions were added into each well followed by its incubation

at 37 for 15 minutes. At the end of the reaction, HRP stop buffer was added and the absorbance signal was measured at OD₄₉₀ as indicated above.

VI. Biochemical assay: The cell lysates for biochemical assays were prepared according to the aforementioned protocol for G- LISA.

a. Gel Electrophoresis: Protein samples were processed with 4X laemmli sample buffer (BioRad, Hercules, CA) complemented with β - mercaptoethanol. Samples were heated at 95°C for ten minutes followed by a quick cycle of centrifugation to remove cell particles. The proteins were then separated in a 12% Sodium dodecyl Sulphate Polyacrylamide Gel Electrophoresis (SDS-PAGE) by using a Mini-Protean electrophoresis apparatus (BioRad, Hercules, CA). Each lane was loaded with 20 μ g of protein or 5 μ l of BioRad molecular weight makers 161-0318. The proteins were electrophoresed by using NuPAGE® MOPS SDS Running Buffer (20X) (Life Technologies, NY) at 40V for 10 minutes followed by a run at 100V for 1 hour. We used Acqua stain protein gel stain (Bulldog Bio, Inc., NH) to stain the gels for 15 minutes. The unstained gels were equilibrated in TBST (Tris Buffer Saline (TBS), 0.1% Tween 20) buffer before using them for Western Blot Transfer.

b. Western Blot Analysis: Separated proteins were then transferred to a 0.45 μ m nitrocellulose membrane in a BioRad Trans Blot Turbo system. The membranes were then blocked for 2 hours with 5% bovine serum albumin in TBST (Tris Buffer Saline (TBS), 0.1% Tween 20) at room temperature. The appropriate primary antibody dilution of either occludin (1:250) (Cell Signaling Technology, Inc. Danvers, MA) or ZO-1 (1:250) (Invitrogen, Carlsbad, CA) was

added for overnight at 4°C. Secondary antibody GAR (Goat anti Rabbit) -HRP (BioRad, Hercules, CA) was added for 2 hours at room temperature. An amplification step was performed using a Blot Amplification module (BioRad, Hercules, CA). After amplification, colorimetric detection was performed using Opti-4CN Substrate Kit (BioRad, Hercules, CA) for 30 minutes. Immunoblots were documented using UVP GelDoc-IT imaging System (UVP, Upland, CA) and quantified with ImageJ software (NIH, USA).

VII. Immuno-staining: Confluent monolayers of Calu-3 cells were seeded on 8 – well tissue culture treated chamber slides (Lab-Tek, Rochester, NY) as mentioned earlier. Morphological changes induced by *Pseudomonas* Elastase in the absence or presence of various inhibitors across the confluent cell monolayers were then analyzed after the cells were stained for F-actin. The cells were fixed with 3.7 % paraformaldehyde in PBS for 10 minutes followed by cell permeabilization step with 0.5% Triton-X 100 in PBS for 5 minutes at room temperature. Finally, the treated cells were incubated with Acti-Stain 555 Fluorescent Phalloidin (Cytoskeleton, Inc., Denver, CO) in PBS for 30 minutes in the dark at room temperature for F- actin visualization. The cells were then washed thrice with PBS. This is followed by counterstaining of cells with 100 nM DAPI (4', 6'-di-amidino-2-phenylindole, Invitrogen, Camarillo, CA). The monolayers were examined under Zeiss LSM 5 Pascal Laser scanning Confocal Microscope equipped with an Axiocam HRc Color Digital Camera (One Zeiss Drive, Thornwood, NY). Photomicrography was performed under 63X with oil and

images were overlaid and pseudo-colored (green –actin) for ease of visualization in LSM software by Zeiss.

Changes in the formation of stress fibers, cell cortex and protrusions such as lamellipodium and filopodium helped to determine and compare the differences in F- Actin organization pattern. Differences in the localization of tight junction proteins were visually observed and documented as well.

VIII. Statistical Analysis: Statistical analysis of the differences between the means was performed with GraphPad Prism 6 (GraphPad Software, San Diego, CA). Results from spectrophotometric analysis of immunological assays such as G-LISA and ELISA and densitometric analysis from Western Blot are evaluated by using ANOVA followed by hoc pairwise comparisons and Dunnett's t-test. Results are presented as means \pm standard deviation and considered significant when p-value < 0.05.

Chapter Three

Results

Activation of RhoA GTPases by Pseudomonas aeruginosa Elastase (PE)

We sought to investigate whether PE alters F-actin structure and organization through activation of RhoA intermediate in Rho-ROCK pathway. We compared the RhoA GTPases activity in cells treated with PE alone to that of the PBS-treated control monolayers. We observed that PE increases the phosphorylation of RhoA proteins significantly over the PBS treated control monolayers *in vitro* (1.787 ± 0.15 vs 1.188 ± 0.17 , $p < 0.05$, $n = 3$). The RhoA GTPase activity in PE treated Calu 3 cells was 50.8% higher than the PBS treated control cells. Further, we analyzed whether inhibitor of RhoA was able to slow down the phosphorylation activity of RhoA proteins induced by PE. Calu-3 cells were pre-treated with RhoA Inhibitor for 120 minutes and later with PE for 5 minutes. Cell lysates at the end of 5 minutes of PE exposure were normalized and analyzed through G-LISA activation Assay in colorimetric format. Spectrophotometric analysis of cell lysates showed that the specific RhoA inhibitor reduced the kinase activity in PE-treated cells by 30.35%. In the experimental setup, a purified phosphorylated RhoA protein was utilized as a positive control as shown in Figure 1. These changes in the phosphorylation state of RhoA Proteins was found to be correlated with the morphological changes in the F-actin molecules as shown in Figure 4.

Figure 1 b depicts the amount of phosphorylated RhoA kinase. The concentration of phosphorylated RhoA proteins was observed to be significantly higher in PE treated monolayers than the PBS treated control cells (1.080 ± 0.13 vs 0.706 ± 0.04 , $p < 0.05$, $n=3$). The amount of PE-induced phosphorylated RhoA protein was as high as the positive control, whereas, Calu-3 monolayers pretreated with RhoA inhibitor reduced the amount of activated kinase significantly (0.49 ± 0.03 .vs 1.080 ± 0.13 , $p < 0.005$, $n=3$).

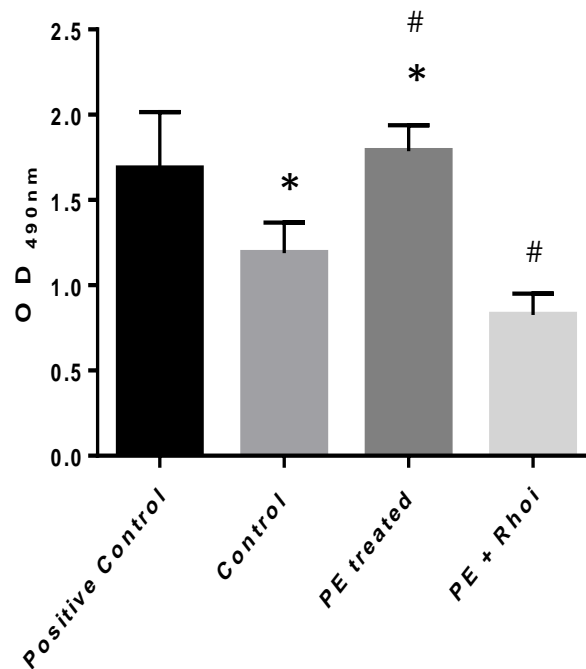


Figure 4a. *Pseudomonas aeruginosa* Elastase induces RhoA GTPase phosphorylation. Confluent monolayers of Calu- 3 were pre- treated with 500ng/ml of RhoA inhibitor for 120 minutes followed by stimulation with 3U/ml of PE for 5 minutes. PE induced RhoA GTPase phosphorylation was measured by G-LISA Small G- Protein Activation Assay. Data is expressed as means \pm standard deviation of triplicate assays. * indicate significant increase ($p=0.003$) in RhoA GTPase phosphorylation in PE treated cells in comparison to PBS-treated control cells. # indicates decrease in RhoA GTPase phosphorylation in RhoA inhibitor treated cells in comparison to PE treated Calu-3 monolayer.

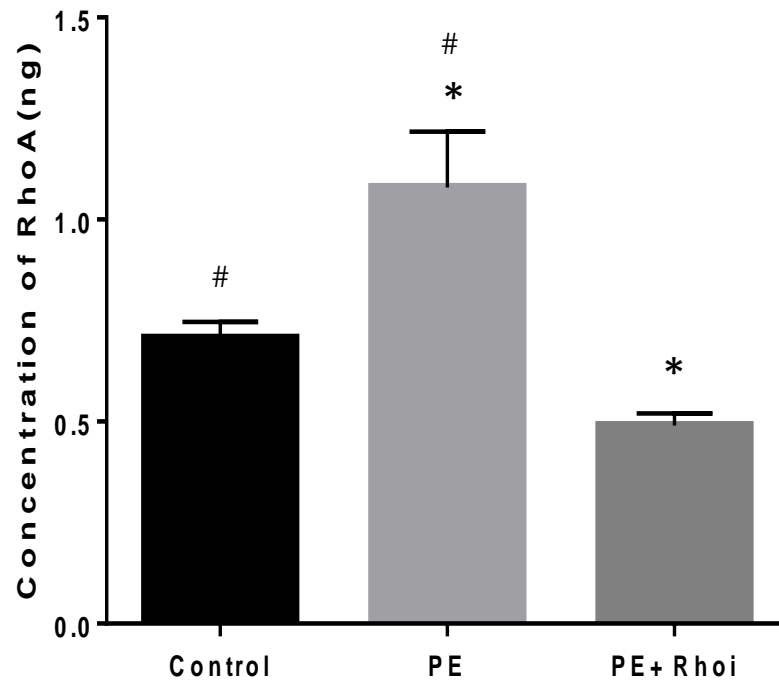


Figure 4b. *Concentration of Phosphorylated RhoA GTPase measured by G-LISA:* Confluent monolayers of Calu- 3 were pre- treated with 500ng/ml of RhoA inhibitor for 120 minutes followed by stimulation with 3U/ml of PE for 5 minutes. Data is expressed as means \pm standard deviation of triplicate assays. # indicate significant increase (<0.001) in RhoA GTPase phosphorylation in PE treated cells in comparison to PBS-treated control cells.* indicates decrease in RhoA GTPase phosphorylation in PE + RhoA inhibitor treated cells in comparison to PE- treated cells.

Inhibition of EGFR/ MAPK signal transduction pathway attenuates PE-induced RhoA GTPase activity

In an effort to understand the mechanism by which PE increases RhoA GTPase activity in Calu-3 cells, we investigated the effect of PE on RhoA GTPase activation in the presence of specific inhibitors for Epidermal Growth Factor Receptor (EGFR) and Mitogen Activated Protein Kinase (MAPK) pathways. We observed that Calu-3 monolayers treated with *P. aeruginosa* elastase significantly increased the amount of active GTP bound RhoA in cell lysates in comparison to the PBS treated control cells (1.839 ± 0.06 VS 1.21 ± 0.12 , $p < 0.05$, $n=3$). In this series of experiments, Calu-3 monolayers were pre-treated with AG1478, a specific EGFR tyrosine kinase inhibitor or U0126, a highly selective inhibitor of MAPK/ERK kinase (ERKi) for 15 minutes. Cells were also pretreated with RhoA inhibitor CTO4 for 120 minutes prior to PE treatment. The monolayers were then exposed to 3 U/ml PE for 5 minutes and the cell lysate were analyzed for RhoA activity by G-ELISA. Similar to our findings shown in Figures 1a and b, PE increase RhoA activity by 51% over the PBS-treated control cells. However, we observed a pronounced loss in RhoA GTPase activity in monolayers pretreated with EGFRi in comparison to cells treated with PE alone (0.9773 ± 0.03 vs 1.839 ± 0.06 , $p < 0.05$, $n=3$). Similarly, cells pre-treated with UO126 showed reduced kinase activity analogous to the EGFRi treatment, wherein the phosphorylation of RhoA proteins was significantly reduced (1.027 ± 0.05 vs 1.839 ± 0.06 , $p < 0.05$, $n=3$). Analysis of cell lysates treated with CTO4 showed similar effect as EGFRi and ERKi. Taken together,

our data indicate that PE, at least in part, activates RhoA kinase via upstream EGFR signaling and downstream MAPK pathways.

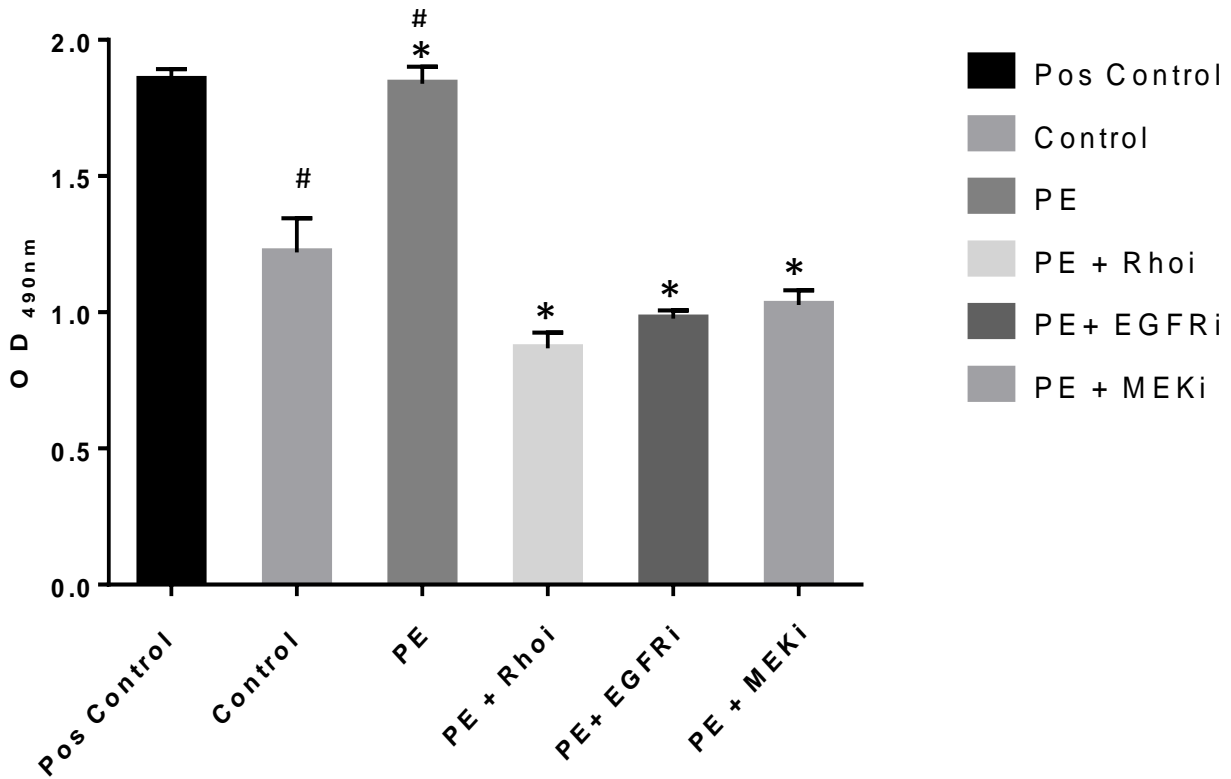


Figure 5. *Signal transduction pathways involved in PE induced RhoA GTPase.* Confluent monolayers of Calu-3 were pre-treated with 500ng/ml of RhoA inhibitor, 1 μ M EGFR inhibitor or 1 μ M of MEK inhibitor for 120 minutes and 15 minutes respectively, followed by stimulation with 3U/ml of PE for 5 minutes. PE induced RhoA GTPase phosphorylation measured by G-LISA Small G- Protein Activation Assay was found to be attenuated in presence of inhibitors. Data is expressed as means \pm standard deviation of triplicate assays. # indicate significant increase ($p=0.05$) in RhoA GTPase phosphorylation in PE treated cells in comparison to PBS-treated control cells. * indicates decrease in RhoA GTPase phosphorylation in various inhibitor treated cells in comparison to PE - treated cells.

Quantitative Measurement of Total RhoA Proteins by ELISA Assay

Enzyme-linked Immunosorbent Assay (ELISA) was used for the quantitative measurement of Total RhoA protein in cell extracts treated with PE in the presence and absence of RhoA inhibitor. Confluent monolayers of Calu-3 were pre-treated with 500ng/ml of RhoA inhibitor followed by stimulation with 3 U/ml of PE for 5 minutes. The amount of total RhoA protein in cell lysates was quantified by spectrophotometric analysis. The amount of Total RhoA protein was observed to be significantly higher in PE treated cells in comparison to PBS treated cells (1.138 ± 0.05 , vs 0.87 ± 0.08 , $p < 0.05$, $n = 3$). Calu-3 monolayer treated with RhoA inhibitor reduced the amount of total RhoA protein to the level of the PBS treated control cells. (Figure 3a).

We analyzed the concentration of Total RhoA protein in cell lysates in the presence of inhibitors specific to EGFR and MAPK pathways to investigate the role of potential upstream and downstream signaling pathways. Confluent monolayers of Calu-3 were pre-treated with 500ng/ml of RhoA inhibitor, 1 μ M EGFR inhibitor AG1478 or 1 μ M of MEK 1&2 inhibitor U0126 for 120 minutes and 15 minutes respectively, followed by stimulation with 3 U/ml of PE for 5 minutes. The amount of total RhoA GTP proteins was reduced by 12.12% in cells pretreated with EGFRi in comparison to cells treated with PE alone. Cells pre-treated with “MEK 1&2 inhibitor UO126” showed results analogous to the EGFRi treatment, wherein the total RhoA protein was reduced by 15.4%. Analysis of cell lysates treated with RhoA inhibitor CTO4, showed similar effect in comparison to EGFRi and ERKi treated cells as shown in Figure 3b. The degree

of increase in total RhoA protein is considerably less than that of active RhoA described above.

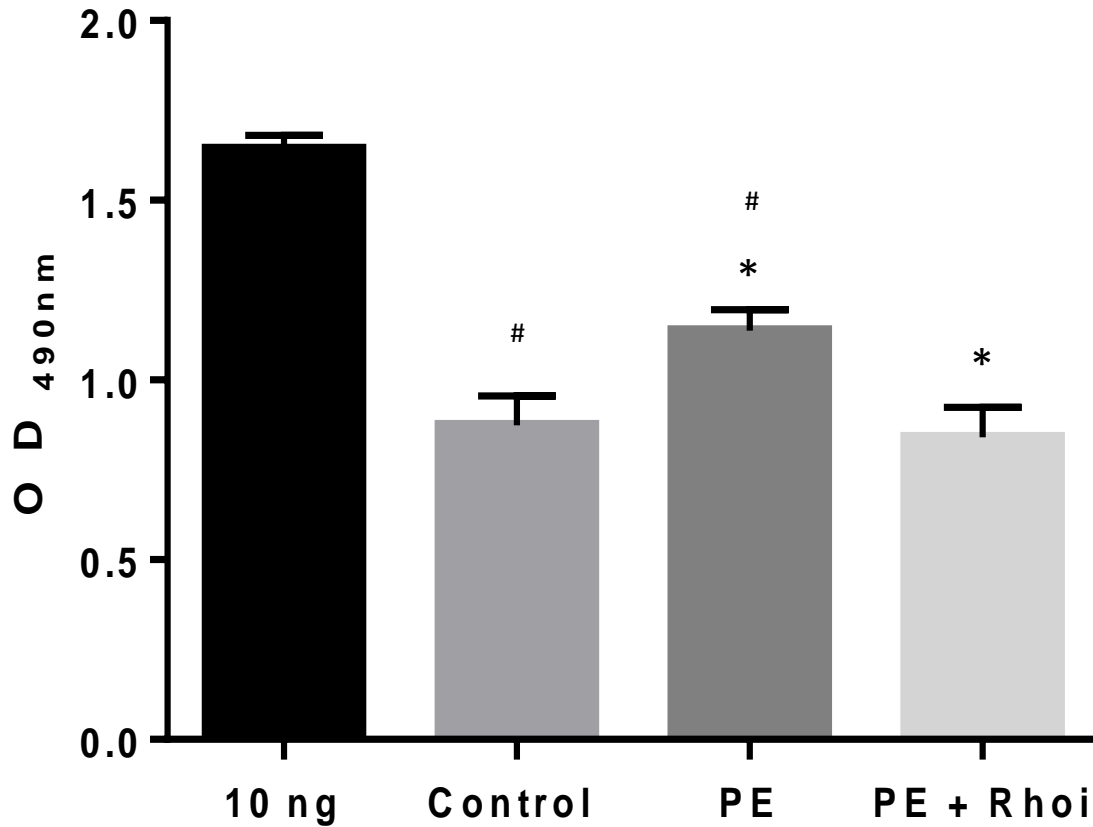


Figure 6a. Concentration of Total RhoA protein in PE induced infection as measured by ELISA Assay. Confluent monolayers of Calu- 3 were pre- treated with 500ng/ml of RhoA inhibitor, was stimulated with 3U/ml of PE for 5 minutes. ELISA measured the total amount of RhoA protein was expressed in cell lysates treated with both PE and PE with RhoA inhibitor. Data is expressed as means \pm standard deviation of triplicate assays. # indicate significant increase ($p < 0.05$) in RhoA GTPase phosphorylation in PE treated cells in comparison to PBS-treated control cells. * indicates decrease in RhoA GTPase phosphorylation in RhoA inhibitor treated cells in comparison to PE- treated cells.

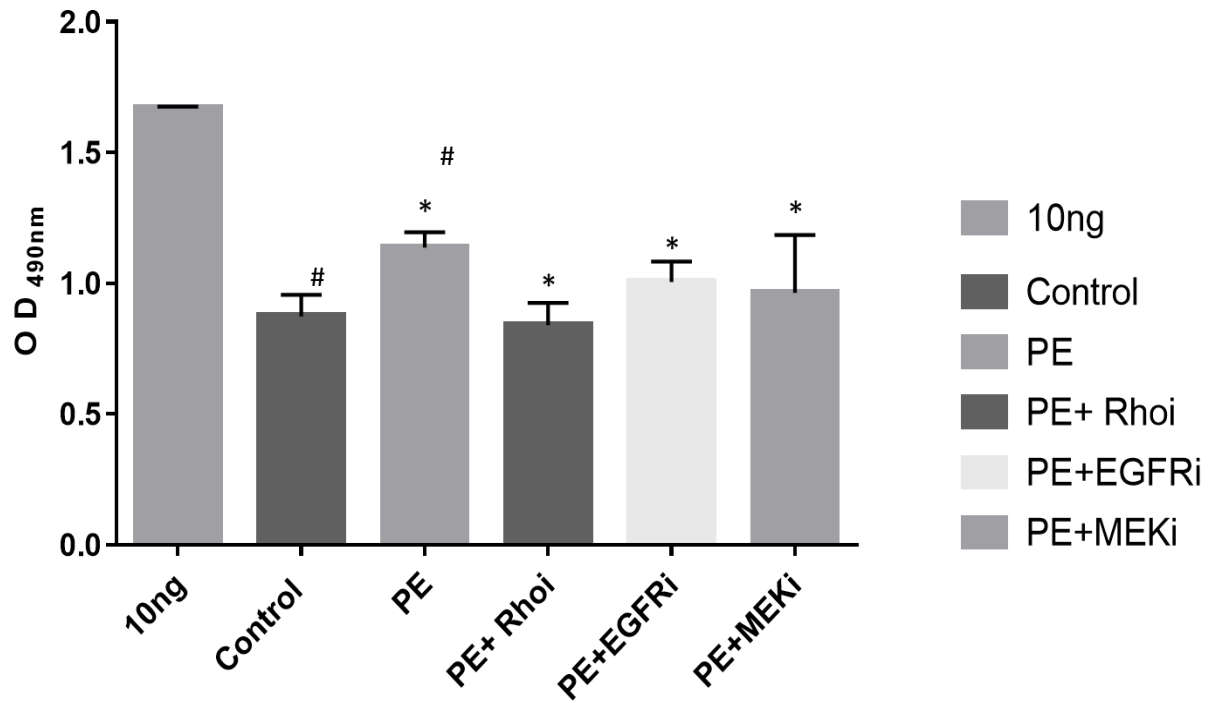


Figure 6b. Concentration of Total RhoA protein in presence of various inhibitors as measured by ELISA Assay: Confluent monolayers of Calu- 3 were pre- treated with 500 ng/ml of RhoA inhibitor, 1 μ M EGFR inhibitor or 1 μ M of MEK inhibitor for 120 minutes and 15 minutes respectively, followed by stimulation with 3 U/ml of PE for 5 minutes. Total amount of PE- induced RhoA protein was measured by ELISA Assay. Data is expressed as means \pm standard deviation of triplicate assays. # indicate significant increase ($p < 0.05$) in total RhoA in cell lysates treated with PE in comparison to PBS-treated control cells. * indicates decrease in the total concentration of RhoA protein in various inhibitor treated cells in comparison to PE- treated cells

Pseudomonas aeruginosa Elastase alters Actin Cytoskeleton Architecture by RhoA Activation

We sought to determine whether the phosphorylation of RhoA proteins by *P. aeruginosa* Elastase induces remodeling of the actin cytoskeleton. We compared F-actin organization in Calu-3 control monolayer to PE treated cells in the presence and absence of specific inhibitors of signaling pathways Rho-ROCK, EGFR, and MAPK. Rhodamine staining of filamentous – actin (F-Actin) followed by its visualization and analysis on LSM 5 Pascal laser scanning confocal microscope revealed that the cells treated with 3 U/ml of PE for 5 min extensively altered the cellular architecture by formation of stress fibers (Figure 4). The PBS- treated cells displayed regular cytoskeletal distribution in cell cortex and peripheries (Figure 4). Pre- treatment with RhoA inhibitor restored the organization of cell cortex and reduced the formation of stress fibers in comparison to PE treated cells (Figure 4) whereas, pre- treatment with MEK and EGFR inhibitor for 15 minutes reduced the effect of PE considerably. The cell peripheries became visible and the amount of stress fibers formation was reduced within the area. Monolayer treated with MEK and EGFR inhibitor induced the formation of other morphological protrusions such as lamellipodium and filopodium

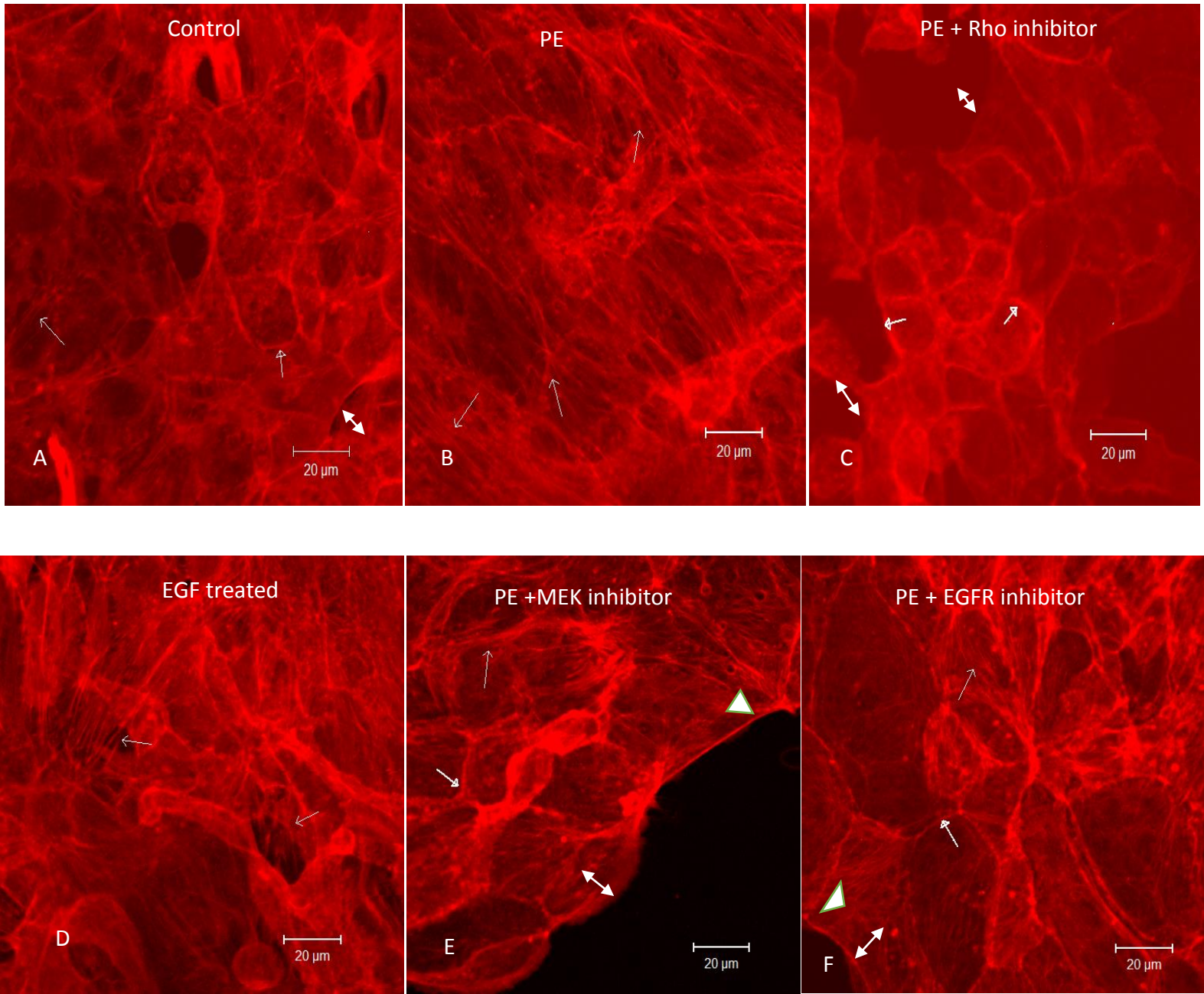


Figure 7. Actin Cytoskeleton architecture is affected by PE induced RhoA GTPase activity. Confluent Calu-3 monolayers were stained for F-actin where narrow arrows indicate formation of stress fibers, bold arrows indicate cell cortex and peripheries and arrow with double heads indicate formation of lamellipodium and triangle indicates filopodium. (A) In PBS treated cells, regular distribution of cell cortex and peripheries along with few stress fibers and lamellipodium was observed. (B) PE treatment (3 U/ml, 5 min) altered the cellular architecture and induced formation of extensive stress fibers and lamellipodium. (C) RhoA inhibitor pre-treated cells restored the organization of cell cortex and regular lamellipodium. (D) EGF treated cells (positive control) caused similar reorganization of actin cytoskeleton by formation of stress fibers. (E) and (F) MEK inhibitor and EGFR inhibitor pre-treated cells reinstated the effect of PE by formation of cell cortex, lamellipodium and filopodium. Images are representative of triplicate assays and scale bar is 20 μm .

Inhibition of RhoA/EGFR/ MAPK pathway affects the expression of ZO-1 tight junctional protein

We next investigated whether PE-induced RhoA activation and cytoskeletal alterations affect expression of TJ protein Zonula Occludens (ZO-1). We observed that exposure to PE for 5 minutes does not reduce the ZO1 expression from the cell lysates. Cell lysates were prepared by the similar protocol followed in G-LISA/ELISA protocols. Western blotting analysis of SDS-PAGE separated proteins was performed using monoclonal mouse anti-ZO1 antibodies. Density of the bands were measured for comparative analysis. PE at 3 U/ml for 5 minutes was unable to induce significant changes in the concentration of ZO-1 protein in the monolayers. The data revealed high ZO-1 expression in cytoplasmic fraction of the cell lysates in response to PE while the cells treated with inhibitors of RhoA, EGFR and MAPK showed a decrease in the ZO-1 expression. The results obtained from the densitometric analysis of the bands were not statistically significant. Beta actin bands indicate equal loading of the samples.

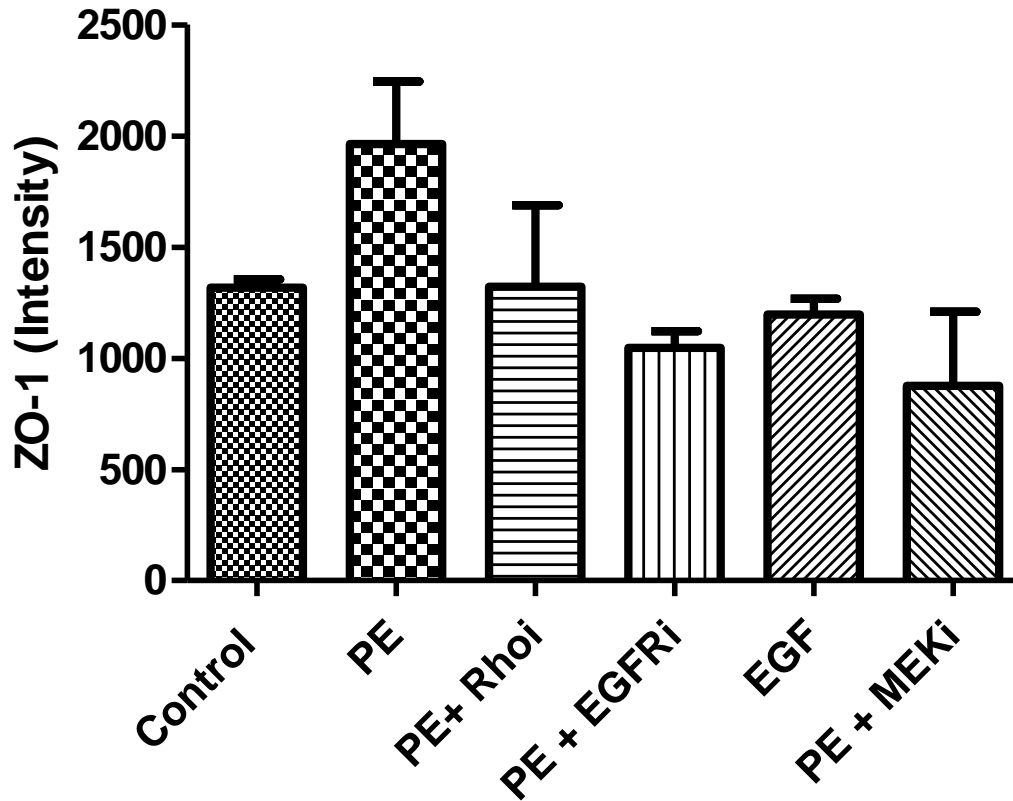
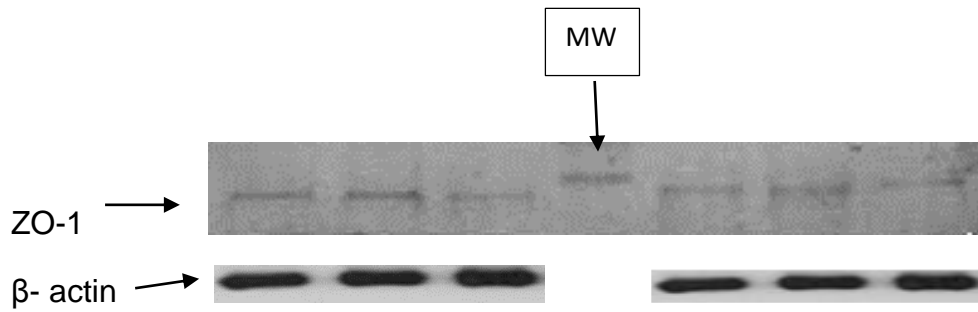


Figure 8. *Expression of ZO-1 is affected by attenuation of RhoA/EGFR and MAPK pathway.* Confluent monolayers of Calu- 3 were pre- treated with 500ng/ml of RhoA inhibitor, 1 μ M EGFR inhibitor or 1 μ M of MEK inhibitor for 120 minutes and 15 minutes respectively, followed by stimulation with 3U/ml of PE for 5 minutes. Proteins separated via SDS PAGE electrophoresis was transferred to Western Blot membrane. PE induces increase in RhoA GTP proteins in comparison to cells treated with inhibitors. The data from densitometry Analysis is observed to be insignificant (>0.05)

Chapter Four

Discussion

Pathogenic bacteria use toxins and proteases to cause tissue damage and they escape from the host defenses through proteolysis of extracellular as well as cell-associated immune effector cells and molecules (95-96). The molecular determinants of the host play an important role in pathogen-host interactions as well. Pulmonary epithelia presents a hostile environment for the antigens and foreign particles. Therefore, human pathogens must possess multiple virulence factors to manipulate host anatomy and physiology including the Immune system. Multiple secreted and cell associated virulence determinants contribute to *P. aeruginosa* pathogenicity. Proteases secreted by *P. aeruginosa* are exemplary in this respect, and even though not all clinical isolates of *P. aeruginosa* produce elastases (40, 45), for those that do, this particular protease proves to be an important candidate for providing the microorganism with immuno evasive capacity.

In this study, we set forth the hypothesis that PE induces remodeling of actin cytoskeleton via activation of RhoA-ROCK signaling pathway. The PE mediated reorganization of the microfilament may depend on multiple signaling pathways including upstream EGFR and downstream MAPK. We addressed this hypothesis using G-LISA and ELISA immunoassays. We utilized specific inhibitors of target signaling pathways to investigate the mechanism of action of PE-induced alteration of cytoskeleton. Further, the morphological changes

induced by PE were evaluated in the absence and presence of specific inhibitors of EGFR and MAPK cascades using fluorescence microscopy.

The data from G-LISA assay show that PE induces phosphorylation of RhoA protein, the first intermediate kinase in Rho-ROCK signaling pathway. The members of Rho family of GTPases act as molecular switches that are known to regulate signal transduction pathways by interconverting between inactive GDP-bound and active GTP-bound conformational states (83). Membrane bound signaling pathways bring Rho proteins to the membrane through the action of specific membrane bound regulatory proteins, guanine nucleotide exchange factors (GEFs). GEF activates RhoA proteins at the membrane by releasing them from GDP bound state for GTP. Membrane bound activated Rho –GTP then binds to effector proteins such as Rho associated Kinase (ROCK) to induce changes in the underlying cytoskeleton. Rho GTPases, in general, mediates various processes in reference to actin cytoskeleton which includes migration, phagocytosis, endocytosis, morphogenesis and cytokinesis. During the process of inflammation via various agents such as cytokines and bacterial products including proteases, rapid disassembly of adherence junctions occurs in conjunction with the remodeling of the F-actin cytoskeleton. The close relationship between the F-actin rearrangement and the epithelial TJ complex reorganization indicates that the Rho proteins might affect the epithelial barrier function through cytoskeletal modification.

Published reports indicate that Rho proteins regulate the assembly and organization of filamentous actin (F-actin) in response to lysophosphatidic acid

(LPA) in a fibroblast cell line (83). Rac was shown to promote the assembly of a peripheral actin meshwork, leading to formation of lamellipodia and membrane ruffles in response to platelet-derived growth factor (PDGF) or insulin (83, 84). Our study indicated that the mechanism of PE-induced pulmonary injury and identify signaling pathways involved. The main objective of this thesis research was to investigate the molecular mechanisms of PE-induced alteration in Calu-3 pulmonary cells cytoskeleton. Herein, we report that the PE increased RhoA GTPase activity significantly within 5 minutes of exposure (Figure 1a). Pretreating the monolayer with RhoA inhibitor significantly reduces the phosphorylation of RhoA Proteins in the presence of *P. aeruginosa* Elastase. The RhoA inhibitor utilized for the study was a highly purified C3 Transferase which is covalently linked to a proprietary cell penetrating moiety via a disulfide bond. These findings therefore suggests that the RhoA GTPase activity is significantly enhanced in presence of PE which may further aid the pathogen in the establishment of epithelial injury in Calu-3 cells.

Enzyme-linked Immuno-sorbent Assay (ELISA) was used for the quantitative measurement of total RhoA protein in cell extracts. This assay was utilized to determine the total amount of RhoA protein which included both the phosphorylated as well as non-phosphorylated kinase. The results from the ELISA assay indicate that PE increases concentration of total RhoA protein as well.

We confirmed our immunoassay data with fluorescence microscopy of the cells labeled with Rhodamine. Fluoresce images indicated that PE causes

extensive restructuring of the underlying actin cytoskeleton. These changes included formation of stress fibers and other distinct morphological structures such as lamellipodium and filopodium. Several studies indicate the importance of RhoA GTPase pathway in reorganization of the F- actin in response to extracellular cues. A number of *in vitro* studies have investigated the effects of microbial toxins and inflammatory mediators on the organization of the epithelial F-actin cytoskeleton. These studies have demonstrated that inflammatory stimuli alter structure of peri-junctional F-actin in conjunction with Adherens Junction Complex (AJC) disassembly (100). Moreover, incubation of colonic and renal epithelial cells with interferon (IFN) (97) or TNF (98) causes reorganization of the peri-junctional F-actin belt into different contractile structures such as apical rings, vacuoles, or stress fiber-like cables. Similar contractile F-actin structures were observed when pulmonary epithelial cells were subjected to hypoxia or treated with transforming growth factor (TGF) (99). We observed that PE induces significant morphological changes in the Calu-3 monolayer by formation of stress fibers, lamellipodium and filopodium. In response to protease such as PE, actin filaments rapidly cross-link at the leading edge of the membrane to form protrusions such as lamellipodium. In some cases, PE causes formation of stress fibers where the contractile fibers in the cell cortex squeezes the cell body forward and the meshwork of actin filaments in the leading edge of cell causes the forward movement of cell. The presence of significant number of stress fibers and other pronounced morphological protrusions in Calu-3 cells within 5 minute of PE exposure suggest that PE causes modification of the actin cytoskeleton via

activation of RhoA GTPase proteins (Figure 5). This finding is supported by the data from the small GTPase activation assays for RhoA GTPase proteins where significant expression of RhoA GTPase proteins was observed in such a short time, a common phenomenon in cell signal transduction process.

As for the molecular mechanism of PE-induced cytoskeleton remodeling in Calu3 lung epithelia, we used specific inhibitors to target signaling pathways of EGFR and MAPK.

We explored the molecular mechanisms that PE exploits to restructure the underlying actin cytoskeleton. Interestingly, inhibition of RhoA GTPase activity by inhibitors of either RhoA, EGFR, or MEK attenuates reorganization of the cytoskeletal architecture induced by PE. Previous studies from our lab indicate that PE induces activation of Protein Kinase C (PKC) signaling pathway through phosphorylation of EGFR, which results in disruption of tight junction proteins, reorganization of the cytoskeleton, and destruction of epithelial barrier function (94). This further suggests that PE might exploit more than one downstream signal transduction cascades in the reorganization of actin cytoskeleton. Further, a cross-talk between the RhoA , EGFR, and MAPK signal transduction pathways might be involved in the pathogenesis of PE induced F- actin assembly and reorganization.

Properties of the epithelium are regulated by adhesive interactions that occur at the cell–cell and cell–matrix contacts by junctional proteins and focal adhesion molecules (101). Epithelial tight junctional complexes are characterized by their dynamic nature and the ability of being constantly remodeled in response to their interactions with external stimuli, such as allergens, pathogens, and commensal bacteria (61, 62). Alteration of this process, however, may result in TJ disassembly and a subsequent increase in cellular permeability. Recent studies have revealed the importance of RhoA GTP binding proteins in the biogenesis, maintenance and regulation of epithelial Tight Junction structure, function and assembly (78). However, the molecular mechanisms by which Rho proteins influence TJs of epithelial cells are not yet clear.

Due to the close association between cytoskeleton and zonula occluden proteins, we investigated the role of PE-induced F-actin alterations on ZO-1 protein expression and organization. We observed a general trend where, ZO-1 protein expression in the cytoplasmic fraction was up-regulated in cell lysates treated with PE. The results obtained from the study did not demonstrate statistically significant changes. On the other hand, the presence of RhoA, EGFR and MEK inhibitors reduced the expression of ZO-1 protein in the first 5 minutes of PE apical exposure, as detected by western blot analysis. We speculate that PE-induced activation of Rho GTPase proteins will affect epithelial barrier function through F-actin-related dislocation of ZO-1 from inner leaflet of the membrane to cytosol, a phenomenon that needs further exploration.

In conclusion, the results from this study indicate that *Pseudomonas* Elastase is capable of quickly activating RhoA GTPase via EGFR/MAPK pathways. Activation of Rho-ROCK pathway resulted in distinct morphological changes in F- actin architecture. The impact of this PE-induced alterations in the anatomy and physiology of tight junctional complex and its implication on the homeostasis of the lungs demands further investigation.

Bibliography

1. Driscoll JA, Brody SL, Kollef MH (2007). The Epidemiology, Pathogenesis and Treatment of *Pseudomonas aeruginosa* Infections. *Drugs*; 67:351-368.
2. Van Delden C, Iglewski BH (1998). Cell-to-cell signaling and *Pseudomonas aeruginosa* infections. *Emerg Infect Dis*. Oct-Dec; 4(4):551-60. Review. PubMed PMID: 9866731; PubMed Central PMCID: PMC2640238.
3. Dunn M, Wunderink RG (1995). Ventilator-associated pneumonia caused by *Pseudomonas* infection [review]. *Clinics in Chest Medicine*; 16:95-109.
4. Brewer SC, Wunderink RG, Jones CB, Leeper KVJ (1996). Ventilator-associated pneumonia due to *Pseudomonas aeruginosa*. *Chest*; 109:1019-29.
5. Chastre J, Fagon JY. Ventilator-associated pneumonia (2002). *Am J Respir Crit Care Med*; 165:867- 903.
6. Sinuff T, Muscedere J, Cook D, Dodek P, Heyland D (2008). Ventilator-associated pneumonia: improving outcomes through guideline implementation. *J Crit Care*; 23:118-25.
7. Knaus WA, Draper EA, Wagner DP, Zimmerman JE (1985). APACHE II: a severity of disease classification system. *Crit Care Med*; 13:818-29.
8. Harris A, Torres-Viera C, Venkataraman L, DeGirolami P, Samore M, Carnieli Y (1999). Epidemiology and clinical outcomes of patients with multiresistant *Pseudomonas aeruginosa*. *Clin Infect Dis*; 28:1128-33.

9. Mirsaiedi M, Peyrani P, Ramirez JA; Improving Medicine through Pathway Assessment of Critical Therapy of Hospital-Acquired Pneumonia (IMPACT-HAP) Investigators. Predicting mortality in patients with ventilator-associated pneumonia: The APACHE II score versus the new IBMP-10 score. *Clin Infect Dis*. 2009 Jul 1; 49(1):72-7.
10. McManus AT, Mason AD Jr, McManus WF, Pruitt BA Jr *Eur J*. (1985). Twenty-five year review of *Pseudomonas aeruginosa* bacteremia in a burn center *Clin Microbiol*. Apr; 4(2):219-23.
11. Rumbaugh, K. P., Griswold, J. A., Iglewski, B. H., & Hamood, A. N. (1999). Contribution of Quorum Sensing to the Virulence of *Pseudomonas aeruginosa* in Burn Wound Infections. *Infection and Immunity*, 67(11), 5854–5862.
12. Gessard C et al. (1850-1925). Classics in infectious diseases. On the blue and green coloration that appears on bandages. *Rev Infect Dis*. 1984 Sep-Oct; 6 Suppl 3():S775-6.
13. Aloush V, Navon-Venezia S, Seigman-Igra Y, Cabili S, Carmeli Y (2006). Multidrug-resistant *Pseudomonas aeruginosa*: risk factors and clinical impact. *Antimicrob Agents Chemother*. Jan; 50(1):43-8.
14. Lambert, P. A. (2002). Mechanisms of antibiotic resistance in *Pseudomonas aeruginosa*. *Journal of the Royal Society of Medicine*, 95(Suppl 41), 22–26. Ramos, J.-L. (ed.) (2004) Volume 1: Genomics, Life Style and Molecular Architecture. New York, NY, USA: Kluwer Academic/Plenum Publishers, pp. 369–571.

15. Schmidt, K.D., Tümmler, B., and Römling, U. (1996) Comparative genome mapping of *Pseudomonas aeruginosa* PAO with *P. aeruginosa* C, which belongs to a major clone in cystic fibrosis patients and aquatic habitats. *J Bacteriol* 178: 85–93.
16. Kiewitz, C., and Tümmler, B. (2000) Sequence diversity of *Pseudomonas aeruginosa*: impact on population structure and genome evolution. *J Bacteriol* 182: 3125–3135.
17. Frimmersdorf, E., Horatzek, S., Pelnikovich, A., Wiehlmann, L. and Schomburg, D. (2010), How *Pseudomonas aeruginosa* adapts to various environments: a metabolomic approach. *Environmental Microbiology*, 12: 1734–1747. doi: 10.1111/j.1462-2920.2010.02253.
18. Stanier, R.Y., Palleroni, N.J., and Doudoroff, M. (1966). The aerobic *Pseudomonads*: a taxonomic study. *J Gen Microbiol* 43: 159–271.
19. Morrison AJ, Wenzel RP (1984). Epidemiology of infections due to *Pseudomonas aeruginosa*. *Rev Infect Dis*; 6: S627–S642.
20. Pollack M, Mandell GL, Bennett JE, Dolin R, eds (2000). *Pseudomonas aeruginosa*. In: Principles and Practice of Infectious Diseases, 5th edn. Philadelphia: Churchill Livingstone: 2310–2335.
21. Sadikot, R. T., T. S. Blackwell, J. W. Christman, and A. S. Prince. (2005). Pathogen-host interactions in *Pseudomonas aeruginosa* pneumonia. *Am. J. Respir. Crit. Care Med.* 171:1209–1223.

22. Knapp, S., M. J. Schultz, and T. van der Poll. (2005). Pneumonia models and innate immunity to respiratory bacterial pathogens. *Shock* 24 (Suppl. 1):12–18.
23. Rossolini GM, Mantengoli E (2005). Treatment and control of severe infections caused by multiresistant *Pseudomonas aeruginosa*. *Clin Microbiol Infect. Suppl* 4:17-32. Review. PubMed PMID: 15953020.
24. McIsaac SM, Stadnyk AW, Lin TJ. (2012). Toll-like receptors in the host defense against *Pseudomonas aeruginosa* respiratory infection and cystic fibrosis. *J. Leukoc. Biol.* 92:977–985.
25. Amiel E, Lovewell RR, O'Toole GA, Hogan DA, Berwin B. (2010). *Pseudomonas aeruginosa* evasion of phagocytosis is mediated by loss of swimming motility and is independent of flagellum expression. *Infect.Immun.* 78:2937–2945.
26. Wolf P, Elsasser-Beile U. (2009). *Pseudomonas* exotoxin A: from virulence factor to anti-cancer agent. *Int. J. Med. Microbiol.* 299:161–176.
27. Liu PV. (1973). Exotoxins of *Pseudomonas aeruginosa*. I. Factors that influence the production of exotoxin A. *J. Infect. Dis.* 128:506–513.
28. Barbieri JT, Sun J. (2004). *Pseudomonas aeruginosa* ExoS and ExoT. *Rev. Physiol. Biochem. Pharmacol.* 152:79–92.
29. Engel J, Eran Y. (2012). Subversion of mucosal barrier polarity by *Pseudomonas aeruginosa*. *Front. Microbiol.* 2:114.

30. Döring G, Parameswaran IG, Murphy TF. (2011). Differential adaptation of microbial pathogens to airways of patients with cystic fibrosis and chronic obstructive pulmonary disease. *FEMS Microbiol. Rev.* 35:124–146.
31. Tingpej P, Smith L, Rose B, Zhu H, Conibear T, Al Nassafi K, Manos J, Elkins M, Bye P, Willcox M, Bell S, Wainwright C, Harbour C. (2007). Phenotypic characterization of clonal and nonclonal *Pseudomonas aeruginosa* strains isolated from lungs of adults with cystic fibrosis. *J. Clin. Microbiol.* 45:1697–1704.
32. Hogardt M, Heesemann J. (2013). Microevolution of *Pseudomonas aeruginosa* to a chronic pathogen of the cystic fibrosis lung. *Curr. Top. Microbiol. Immunol.* 358:91–118.
33. Bleves S, Viarre V, Salacha R, Michel GP, Filloux A, Voulhoux R. (2010). Protein secretion systems in *Pseudomonas aeruginosa*: a wealth of pathogenic weapons. *Int. J. Med. Microbiol.* 300:534–543.
34. Lau GW, Hassett DJ, Britigan BE. (2005). Modulation of lung epithelial functions by *Pseudomonas aeruginosa*. *Trends Microbiol.* 13:389–397.
35. Passador L, Iglewski BH (1995). Quorum sensing and virulence gene regulation in *Pseudomonas aeruginosa*. In: Roth JA, editor. *Virulence mechanisms of bacterial pathogens*. 2nd ed. Washington: American Society for Microbiology. p. 65-78.
36. Kernacki KA, Hobden JA, Hazlett LD, Fridman R, Berk RS (1995). In vivo bacterial protease production during *Pseudomonas aeruginosa* corneal

- infection [published erratum appears in Invest Ophthalmol Vis Sci 1995; 36:1947]. Invest Ophthalmol Vis Sci; 36:1371-8.
37. Howe TR, Iglewski BH (1984). Isolation and characterization of alkaline protease-deficient mutants of *Pseudomonas aeruginosa* in vitro and in a mouse eye model. Infect Immun; 43:1058-63.
38. Galloway DR (1991). *Pseudomonas aeruginosa* elastase and elastolysis revisited: recent developments. Mol Microbiol; 5: 2315-21.
39. Kessler E, Safrin M (1988). Synthesis, processing, and transport of *Pseudomonas aeruginosa* elastase. J Bacteriol; 170:5241-5247.
40. Saulnier JM, Curtil FM, Duclos MC, Wallach JM (1989). Elastolytic activity of *Pseudomonas aeruginosa* elastase. Biochim Biophys Acta.; 995:285-290.
41. Hamdaoui A, Wund-Bisseret F, Bieth JG (1987). Fast solubilization of human lung elastin by *Pseudomonas aeruginosa* elastase. AmRev Respir Dis.; 135:860-863.
42. Heck LW, Morihara K, McRae WB, Miller EJ (1986). Specific cleavage of human type III and IV collagens by *Pseudomonas aeruginosa* elastase. Infect Immun.; 51:115-118.
43. Schmidtchen A, Holst E, Tapper H, Bjorck L (2003). Elastase-producing *Pseudomonas aeruginosa* degrade plasma proteins and extracellular products of human skin and fibroblasts, and inhibit fibroblast growth. Microbial Pathogenesis; 34:47-55.

44. DeBelle L, Tamburro AM (1999). Elastin: molecular description and function. *The International Journal of Biochemistry & Cell Biology*; 31:261-272.
45. Crouch, E. C. (1998). Collectins and pulmonary host defense. *Am. J. Respir. UGA stop codon by multiple suppressions and translational reading gaps.* *Cell Mol. Biol.* 19:177–201.
46. Wright JR (1997). Immuno-modulatory functions of surfactant. *Physiol. Rev.* 77:931–962. (Review)
47. 3. Medzhitov, R., and C. A. Janeway, Jr. (1997). Innate immunity: impact on the adaptive immune response. *Curr. Opin. Immunol.* 9:4–9.
48. Mariencheck WI, Alcorn JF, Palmer SM, Wright JR (2003). *Pseudomonas aeruginosa* elastase degrades surfactant proteins A and D. *Am J Respir Cell Mol Biol.* Apr; 28(4):528-37.
49. Azghani AO, Connelly JC, Peterson BT, Gray LD, Collins ML, Johnson AR (1990). Effects of *Pseudomonas aeruginosa* elastase on alveolar epithelial permeability in guinea pigs. *Infect Immun* 58:433–438
50. Peterson BT, Collins ML, Gray LD, Azghani AO (1992). Aerosolized *Pseudomonas* elastase and lung fluid balance in anesthetized sheep. *J Appl Physiol* 72:1927–1933
51. Azghani AO (1996). *Pseudomonas aeruginosa* and epithelial permeability: role of virulence factors elastase and exotoxin A. *Am J Respir Cell Mol Biol* 15:132–140

52. Azghani AO, Connelly JC, Peterson BT, Gray LD, Collins ML, Johnson AR (1990). Effects of *Pseudomonas aeruginosa* elastase on alveolar epithelial permeability in guinea pigs. *Infect Immun.* Feb;58 (2):433-8.
53. Pavlovskis, O. R., & Wretling, B. (1979). Assessment of protease (elastase) as a *Pseudomonas aeruginosa* virulence factor in experimental mouse burn infection. *Infection and Immunity*, 24(1), 181–187.
54. Hoiby N (1974) *Pseudomonas aeruginosa* infection in cystic fibrosis. Relationship between mucoid strains of *Pseudomonas aeruginosa* and the humoral immune response. *Acta Pathol Microbiol Scand B* 82:551–558
55. Klinger JD, Straus DC, Hilton CB, Bass JA (1978) Antibodies to proteases and exotoxin A of *Pseudomonas aeruginosa* in patients with cystic fibrosis: demonstration by radioimmunoassay. *J Infect Dis* 138:49–58
56. Ivanov, A. I., Parkos, C. A., & Nusrat, A. (2010). Cytoskeletal Regulation of Epithelial Barrier Function during Inflammation. *The American Journal of Pathology*, 177(2), 512–524.
57. Chignard M, Balloy V (2000). Neutrophil recruitment and increased permeability during acute lung injury induced by lipopolysaccharide. *Am J Physiol Lung Cell Mol Physiol*, 279:L1083–L1090
58. Coyne CB, Vanhook MK, Gambling TM, Carson JL, Boucher RC, Johnson LG (2002). Regulation of airway tight junctions+ by proinflammatory cytokines. *Mol Biol Cell*, 13:3218–3234
59. Holgate ST (2007). Epithelium dysfunction in asthma. *J Allergy Clin Immunol*, 120:1233–1244

60. Knight DA, Holgate ST (2003). The airway epithelium: structural and functional properties in health and disease. *Respirology*, 8:432–446
61. Harhaj N, Antonetti D (2004). Regulation of tight junctions and loss of barrier function in pathophysiology. *Int J Biochem Cell Biol*; 36: 1206–1237.
62. Madara, J. L. (1998). Regulation of the movement of solutes across tight junctions. *Ann. Rev. Physiol.* 60, 143-159.
63. Madara JL, Pappenheimer JR (1987). Structural basis for physiological regulation of paracellular pathways in intestinal epithelia. *J Membr Biol*; 100: 149–164.
64. Walsh SV, Hopkins AM, Nusrat A (2000). Modulation of tight junction structure and function by cytokines. *Adv Drug Deliv Rev*; 41:303–313.
65. Atisook K, Carlson S, Madara JL (1990). Effects of phlorizin and sodium on glucose-elicited alterations of cell junctions in intestinal epithelia. *Am J Physiol Cell Physiol*; 258: C77–C85.
66. Lucas R, Verin AD, Black SM, Catravas JD (2009). Regulators of endothelial and epithelial barrier integrity and function in acute lung injury. *Biochem Pharmacol*, 77:1763–1772
67. Swindle EJ, Collins JE, Davies DE (2009). Breakdown in epithelial barrier function in patients with asthma: identification of novel therapeutic approaches. *J Allergy Clin Immunol*, 124:23–34
68. Kon Y, Tsukada H, Hasegawa T, Igarashi K, Wada K, Suzuki E, Arakawa M, Gejyo F (1999). The role of *Pseudomonas aeruginosa* elastase as a

- potent inflammatory factor in a rat air pouch inflammation model. *FEMS Immunol Med Microbiol.* Aug 15; 25(3):313-21. PubMed PMID: 10459586.
69. Azghani AO, Bedinghaus T, Klein R (2000). Detection of elastase from *Pseudomonas aeruginosa* in sputum and its potential role in epithelial cell permeability. *Lung*; 178(3):181-9. PubMed PMID: 10871436.
70. Balda, M. S., L. Gonzalez-Mariscal, K. Matter, M. Cereijido, and J. M. Anderson (1993). Assembly of the tight junction: the role of diacylglycerol. *J. Cell Biol.* 123: 293–302.
71. Citi, S (1992). Protein kinase inhibitors prevent dissociation induced by low extracellular calcium in MDCK epithelial cells. *J. Cell Biol.* 117: 169–178.
72. Nigam, S. K., N. Denisenko, E. Rodriguez-Boulan, and S. Citi (1991). The role of phosphorylation in development of tight junctions in cultured renal epithelial (MDCK) cells. *Biochem. Biophys. Res. Commun.* 181: 548–553.
73. Nilsson, M., H. Fagman, and L. E. Ericson (1996). Ca²⁺-dependent and Ca²⁺-independent regulation of the thyroid epithelial junction complex by protein kinases. *Exp. Cell Res.* 225: 1–1.
74. Denker, B. M., C. Saha, S. Khawaja, and S. K. Nigam (1996). Involvement of a heterotrimeric G protein α subunit in tight junction biogenesis. *J. Biol. Chem.* 271: 25750–25753.
75. Balda, M. S., L. Gonzalez-Mariscal, M. Macias-Silva, M. E. Torres-Marquez, J. A. Garcia Sainz, and M. Cereijido (1991). Assembly and sealing of tight junctions: possible participation of G- proteins,

phospholipase C, protein kinase C and calmodulin. *J. Membr. Biol.* 122: 193–202.

76. Nusrat, A., M. Giry, J. R. Turner, S. P. Colgan, C. A. Parkos, D. Carnes, E. Lemichez, P. Boquet, and J. L. Madara (1995). Rho protein regulates tight junctions and perijunctional actin organization in polarized epithelia. *Proc. Natl. Acad. Sci. USA* 92: 10629–10633.
77. Rodewald, R. S., S. B. Newman, and M. J. Karnovsky (1976). Contraction of isolated brush borders from the intestinal epithelium. *J. Cell Biol.* 70: 541–554.
78. Rojas, A.M., Fuentes, G., Rausell, A. and Valencia, A. (2012) The Ras superfamily: evolutionary tree and role of conserved amino acids. *J. Cell Biol.* 196, 189–201
79. Madaule, P. and Axel, R. (1985) A novel ras-related gene family. *Cell* 41, 31–40
80. Hall, A. (1998) Rho GTPases and the actin cytoskeleton. *Science* 279, 509–514
81. Ridley, A.J. and Hall, A. (1992). The small GTP-binding protein rho regulates the assembly of focal adhesions and actin stress fibers in response to growth factors. *Cell* 70, 389–399
82. Ridley, A.J., Paterson, H.F., Johnston, C.L., Diekmann, D. and Hall, A. (1992). The small GTP-binding protein rac regulates growth factor-induced membrane ruffling. *Cell* 70, 401–410

83. Jou TS, Schneeberger EE, Nelson WJ (1998). Structural and functional regulation of tight junctions by RhoA and Rac1 small GTPases. *J Cell Biol*; 142:101–115.
84. Jou TS, Nelson WJ (1998). Effects of regulated expression of mutant RhoA and Rac1 small GTPases on the development of epithelial (MDCK) cell polarity. *J Cell Biol*; 142:85–100.
85. Roudabush, F. L., Pierce, K. L., Maudsley, S., Khan, K. D. & Luttrell, L. M. (2000). Transactivation of the EGF receptor mediates IGF-1-stimulated Shc phosphorylation and ERK1/2 activation in COS-7 cells. *J Biol Chem* 275, 22583–22589.
86. Dong J, Opresko LK, Dempsey PJ, et al (1999). Metalloprotease-mediated ligand release regulates autocrine signaling through the epidermal growth factor receptor. *Proc Natl Acad Sci USA*;96:6235–40.
87. O'Hackel P, Zwick E, Prenzel N, et al (1999). Epidermal growth factor receptors: critical mediators of multiple receptor pathways. *Curr Opin Cell Biol*;11: 184–9.
88. Klapper L, Kirschbaum MH, Sela M, et al (2000). Biochemical and clinical implications of the erbB/HER signaling network of growth factor receptors. *Adv Cancer Res*;77: 25–79.
89. Takeyama K, Jung B, Shim JJ, et al (2001). Activation of epidermal growth factor receptors is responsible for mucin synthesis induced by cigarette smoke. *Am J Physiol Lung Cell Mol Physiol*;280: L165–72.

90. Takeyama K, Dabbagh K, Shim JJ, et al (2000). Oxidative stress causes mucin synthesis via transactivation of epidermal growth factor receptor: role of neutrophils. *J Immunol*;164: 1546–52.
91. A.S. Dhillon, S. Hagan, O. Rath, W. Kolch (2007). MAP kinase signaling pathways in cancer *Oncogene*, 26, pp. 3279–3290
92. Curtis A. Clark, Lauren K. Thomas, and Ali O. Azghani (2011). Inhibition of Protein Kinase C Attenuates *Pseudomonas aeruginosa* Elastase–Induced Epithelial Barrier Disruption", *American Journal of Respiratory Cell and Molecular Biology*, Vol. 45, No. 6 , pp. 1263-1271.
93. Lahteenmäki, K., S. Edelman, and T. K. Korhonen. (2005). Bacterial metastasis: the host plasminogen system in bacterial invasion. *Trends Microbiol.*13:79–85.
94. Maeda, H., and T. Yamamoto. (1996). Pathogenic mechanisms induced by microbial proteases in microbial infections. *Biol. Chem. Hoppe-Seyler* 377: 217–226.
95. Youakim A, Ahdieh M (1999). Interferon decreases barrier function in T84 cells by reducing ZO-1 levels and disrupting apical actin. *Am J Physiol*, 276:G1279–G1288
96. Kakiashvili E, Speight P, Waheed F, Seth R, Lodyga M, Tanimura S, Kohno M, Rotstein OD, Kapus A, Szaszi K (2009). GEF-H1 mediates tumor necrosis factor induced Rho activation and myosin phosphorylation:

role in the regulation of tubular paracellular permeability. *J Biol Chem*, 284:11454–11466

97. Bouvry D, Planes C, Malbert-Colas L, Escabasse V, Clerici C (2006). Hypoxia-induced cytoskeleton disruption in alveolar epithelial cells. *Am J Respir Cell Mol Biol*, 35:519–527
98. Madara JL, Moore R, Carlson S (1987). Alteration of intestinal tight junction structure and permeability by cytoskeletal contraction. *Am J Physiol*, 253:C854–C861
99. Ivanov, A. I., Parkos, C. A., & Nusrat, A. (2010). Cytoskeletal Regulation of Epithelial Barrier Function During Inflammation. *The American Journal of Pathology*, 177(2), 512–524. doi:10.2353/ajpath.2010.100168
100. Aktories, K., & Barbieri, J. T. (2005). Bacterial cytotoxins: targeting eukaryotic switches. *Nature Reviews Microbiology*, 3(5), 397-410.
101. Blanchoin, L., Boujemaa-Paterski, R., Sykes, C., & Plastino, J. (2014). Actin dynamics, architecture, and mechanics in cell motility. *Physiological reviews*, 94 (1), 235-263.